Characterization of an L-Ascorbate Catabolic Pathway with Unprecedented Enzymatic Transformations

Tyler M. M. Stack, Katelyn N. Morrison, Thomas M. Dettmer, Brendan Wille, Chan Kim, Ryan Joyce, Madison Jermain, Yadanar Than Naing, Khadija Bhatti, Brian San Francisco, Michael S. Carter, John A. Gerlt

Supplementary Data

Table of Contents

Experimental Section

General reagents and methods

All chemicals were purchased from Sigma-Aldrich (St. Louis, MO) except where otherwise noted. 1-[^{13}C]-L-ascorbic acid and DMSO-d_6 were purchased from Cambridge Isotopes and 2-[^{13}C]-L-ascorbic acid was purchased from Omicron Biochemicals. The synthesis and purification of L-lyxonate and other sugar acids has been previously described.[1] Ascorbate oxidase from *Cucurbita* sp., malate dehydrogenase and phosphoenolpyruvate carboxylase (microbial) was purchased from Sigma-Aldrich. Primers were ordered from Integrated DNA Technologies. Plasmid constructs were verified through DNA sequencing performed by ACGT. Thermocycling was performed on a Bio-Rad DNA Engine Thermal cycler (Hercules, CA). Gel extraction of PCR products was performed using the Qiagen Gel Purification Kit (Hilden, Germany). Gel extraction of digested plasmid was performed using a Bio-Rad Freeze 'N Squeeze Kit (Hercules, CA). DNA and protein concentrations were

determined using a NanoDrop 2000 UV-Vis Spectrophotometer (Thermo Fisher Scientific, Waltham, MA) using predicted enzyme extinction coefficients at 280 nm as calculated by ProtParam (https://web.expasy.org/protparam/). The concentration of ClxD was estimated using Bio-Rad Protein Assay (Hercules, CA) according to the manufacturer's protocols and bovine serum albumin (New England Biolabs, Ipswitch, MA) as a standard. Plasmid purification was performed using a Qiagen QIAprep Spin Miniprep Kit (Hilden, Germany). Genomic DNA purification was performed using a Qiagen DNeasy Blood & Tissue Kit (Hilden, Germany). Affinity purification was performed using hand-packed disposable columns containing HisPur Ni-NTA resin (Thermo Fisher Scientific, Waltham, MA). Purity was determined by SDS-PAGE using Bio-Rad 4-20% Mini-PROTEAN TGX Precast SDS-PAGE gels (Hercules, CA). Proteins were concentrated and buffer exchanged using Millipore 10 kDa molecular weight cut off cellulose membrane centrifugal filter units (Darmstadt, Germany).

NEB5α competent *E. coli* (New England BioLabs, Ipswitch, MA) was used for plasmid assembly. NEB5α or DH5α was used for plasmid production and purification. Rosetta2 (DE3) (Novagen, now Sigma-Aldrich, St. Louis, MO) was used for heterologous protein expression. Cells were transformed with plasmids by chemical transformation or electroporation.

NMR spectra were recorded with a 600 MHz Agilent NMR using a ^{1}H-^{19}F/^{15}N-^{31}P probe. NMR spectra were obtained in protonated buffer containing 5% DMSO-d_6 using solvent peak suppression unless otherwise stated. Chemical shifts are reported in parts per million (ppm) using solvent reference as internal standard (for ^{1}H, DMSO-d_6 = 2.50 ppm, for ^{13}C, DMSO-d_6 = 39.5 ppm).

Enzyme assays were performed with a UV-visible spectrophotometer (Varian CARY 300 Bio) using a 1 cm quartz cuvette or with a plate reader (TECAN Infinite 200 Pro) using Thermo Fisher Nunc MicroWell 96-Well Microplates. Kinetic modeling and nonlinear regression data fitting were performed using KinTek Explorer Pro (Austin, TX) or Mathematica 11.3 (Champaign, IL).

Bacterial Strains and Growth Conditions
Escherichia coli strains (DH5α, S17, Rosetta2(DE3) [Novagen, now Sigma-Aldrich, St. Louis, MO], and NEB5α [New England BioLabs, Ipswitch, MA]) were grown shaking aerobically at 37 ^{o}C in LB broth or on LB plates with 100 µg/mL of amplicillin, 34 µg/mL chloramphenicol, or 50 µg/mL kanamycin when necessary.

Ralstonia eutropha H16 (DSM-428) and its derived strains were grown shaking aerobically at 30 ^{o}C in LB or in defined media (per liter: 50 mL 20X Salts [20 g NH_4Cl, 6 g $MgSO_4 \cdot 7H_2O$, 3 g KCl, 0.1 g $CaCl_2 \cdot 2H_2O$, 0.05 g $FeSO_4 \cdot 7H_2O$], 50 mL 20X Phosphate Buffer pH 7.0 [500 mM KH_2PO_4 mixed with 500 mM Na_2HPO_4 until pH 7.0], 1 mL 1000X Trace Element Solution [per liter: 0.5 g NaEDTA, 0.3 g $FeSO_4 \cdot 7H_2O$, 3 mg $MnCl_2 \cdot 4H_2O$, 5 mg $CoCl_2 \cdot 6H_2O$, 1 mg $CuCl_2 \cdot 2H_2O$, 2 mg $NiCl_2 \cdot 6H_2O$, 3 mg $Na_2MoO_4 \cdot 2H_2O$, 5 mg $ZnSO_4 \cdot 7H_2O$, 2 mg H_3BO_3], 1 mL 1000X vitamin solution [per L: 0.1 g cyanocobalamin, 0.3 g pyridoxamine-2 HCL, 0.1 g Ca-D-pantothenate, 0.2 g thiamine dichloride, 0.2 g nicotinic acid, 0.02 g D-biotin], and 900 mL H_2O) with 300 µg/mL kanamycin as necessary and with 10 mM of indicated carbon sources. Growth was observed as the absorbance (optical density, OD) of 300 µL cultures at 600 nm in 96-well plates in a SpectraMax i3 (Molecular Devices, San Jose, CA) plate reader. Precultures were grown in rich media to late exponential phase before cells were washed via centrifugation and resuspension in carbonless defined media. Washed cells were diluted in defined media with indicated carbon sources 50 to 200-fold to generate cultures with initial ODs ~0.08.

Construction of rRNA-depleted, strand-specific RNAseq libraries
Construction of libraries and sequencing on the Illumina HiSeq 4000 were performed at the Roy J. Carver Biotechnology Center at the University of Illinois at Urbana-Champaign. One microgram of purified DNAsed total RNA was used for library preparation. Bacterial ribosomal RNAs were removed with the Ribozero Bacteria kit (Illumina). The rRNA-depleted RNAs were converted into individually barcoded RNAseq libraries with the TruSeq Stranded Total RNASample Prep kit (Illumina, CA). The adaptor-ligated double-stranded cDNAs were amplified by PCR for 8 cycles with the Kapa HiFi polymerase (Kapa Biosystems, MA) to reduce the likeliness of multiple identical reads due to preferential

amplification. The final libraries were quantitated with Qubit (ThermoFisher, MA) and the average cDNA fragment sizes were determined on a Fragment Analyzer. The libraries were diluted to 10 nM and further quantitated by qPCR on a CFX Connect Real-Time qPCR system (Bio-Rad, Hercules, CA) for accurate pooling of barcoded libraries and maximization of number of clusters in the flowcell.

Sequencing on a HiSeq 2500
The pooled barcoded libraries were multiplexed and loaded on an 8-lane flowcell for cluster formation and sequenced on an Illumina HiSeq 2500. The libraries were sequenced from one end of the fragments for a total of 100bp using a HiSeq SBS sequencing kit version 4. Fastq files were generated and demultiplexed with the bcl2fastq v2.17.1.14 Conversion Software (Illumina).

Isolation and Complementation of Markerless Deletion Strains of *R. eutropha*
Deletions removed in-frame portions of the respective coding regions without introducing exogenous sequence. Fragments of 1000 bp of regions flanking the targeted coding region were amplified by PCR (see Table S5 for primers) using PrimeStar GXL (TaKaRa, Mountain View, CA). Each fragment contained ≥27 bp of the coding region and preserved the reading frame of the coding region. Using Gibson cloning (New England Biolabs, Ipswitch, MA), the fragments were assembled with pK18mobsacB[2] digested with *Xba*I/*Bam*HI. The plasmid was transferred into *R. eutropha* via conjugation with S17 transformed with the plasmid. Single crossover strains were isolated as kanamycin resistant on defined media plates. Colonies were additionally streaked for isolation on LB plates with kanamycin. Cells from single colonies were incubated in nonselective LB broth until OD ~ 0.8. A 100 µL aliquot of a 100-fold dilution of the culture was plated on LB plates containing 10% sucrose. Double crossover strains were identified as kanamycin sensitive after colonies were patched on LB plates with and without kanamycin. Wild type revertants were distinguished from mutants by comparing sizes of colony PCR products generated using primers that directed amplification across the deleted region. Mutant genotypes were confirmed by PCR amplifying and sequencing the entire region of the genome that was available for recombination with the fragments contained on the corresponding plasmid.

Phenotypes of mutant strains were complemented by inserting a promoter region and a corresponding coding region into pBBR1MCS2.[3] Promoters were chosen as the upstream fragments of the gene clusters that contained each corresponding gene (see Table S5 for primers and plasmid identities). Promoters and coding regions were amplified with PrimeStar GXL (TaKaRa, Mountain View, CA) and assembled into *Xba*I/*Bam*HI-digested pBBR1MCS2 using Gibson assembly cloning (New England Biolabs, Ipswitch, MA). Molecular cloning of complementation plasmids was performed with NEB5α. Plasmids was transferred into *R. eutropha* strains via conjugation with S17 transformed with the plasmid.

Gene Cloning and Heterologous Expression
Gene inserts were amplified from *R. eutropha* genomic DNA, using the primers listed in Table 2 and Phusion DNA polymerase (New England BioLabs, Ipswitch, MA) following the manufacturer's protocol. These gene inserts were cloned into pET15b by linearizing pET15b through double digestion using *Nde*I and *Bam*HI (New England BioLabs, Ipswitch, MA), and then using Gibson Assembly Master Mix (New England BioLabs, Ipswitch, MA) following the manufacturer's protocols. Correct assembly was verified through DNA sequencing.

Proteins were heterologously expressed in *E. coli* strain Rosetta2 (DE3). Cells were transformed with insert-containing pET15b expression plasmids, and 5 mL LB starter cultures (supplemented with 100 ug/mL ampicillin and 33 ug/mL chloramphenicol) were grown at 37 °C overnight. Proteins were then expressed using Autoinduction media using the suggested adaptation for cold expression.[4] Briefly, ZYM-5052 media was prepared as suggested except for the expression of ClxL, which required 1× metal mix in place of the suggested 0.2× metal mix. All media was made with appropriate antibiotics. 1 mL of overnight culture was added to 1000 mL autoinduction media in 4 L erlenmyer flasks. The shaking cultures (220 rpm) were initially grown 4-5 h at 37 °C. After this initial growth period, culture temperature was dropped to 17 °C and cultures incubated a further 48 hr. Cultures were spun for 20 min at 4,000 × g and the pellets stored at -20 °C. This method generates 16-18 g of cells per 1 L of media.

Protein Purification
The frozen cells (~33 g) were resuspended in Ni-NTA lysis buffer (~120 mL) (50 mM sodium phosphate pH 8, 300 mM NaCl, 20 mM imidazole, 5 mg/mL lysozyme) and incubated on ice for 30 min. Cells were lysed by sonication (Fisher Scientific 550 Sonic Dismembrator) for 1 s on, 4 s off, at 20% power max, for 5 min of total "on" sonication. The lysate was cleared by centrifugation at 12,000 x g for 30 min at 4 °C.

The clarified supernatant containing the His-tagged protein was applied to 5 mL of Ni-NTA resin previously equilibrated with Ni-NTA binding buffer (50 mL) (50 mM sodium phosphate pH 8, 300 mM NaCl, 20 mM imidazole). After equilibration of the Ni-NTA resin with the clarified supernatant on a rocking platform for 30 min, the mixture was added to a disposable column, and the flow-through was discarded. Then the column was washed with Ni-NTA binding buffer (~100 mL) until no further protein was detected in the flow-through. The bound protein was eluted from the column using Ni-NTA elution buffer (50 mM sodium phosphate pH 8, 300 mM NaCl, 250 mM imidazole). Pure fractions were determined by SDS-PAGE and pooled. Proteins were concentrated and buffer exchanged using a centrifugal filter unit into 20 mM sodium phosphate pH 7.2 buffer for general storage. Purified enzyme ClxD was instead exchanged into 100 mM sodium phosphate pH 6.8 for greater stability. For further purification before kinetics, enzymes were added to 80 mL of DEAE resin equilibrated with 20 mM sodium phosphate pH 7.2, using a gradient from 0-1 M NaCl (constant buffer pH and concentration) over 800 mL to elute proteins from the column, using 10 mL fractions. Proteins were tested for purity and concentrated as described above.

LyxD Sugar Acid Dehydratase screen
LyxD was screened for acid sugar dehydration activity with the four hexonates (L-gulonate, L-idonate, L-galactonate, and L-talonate) and the two pentonates (L-lyxonate and L-xylonate) that share identical stereochemistry with L-ascorbate, using the semicarbazide assay.[1] The reaction solutions contained 50 mM Tris-HCl at pH 7.9, 10 mM $MgCl_2$, 10 mM acid sugar, and either 0.4 µM LyxD or an equivalent volume of buffer. The reactions (50 µL) were performed in 1.7 mL microcentrifuge tubes and were incubated at 25 °C for 16 h. A 350 µL aliquot of the semicarbazide reagent (1% semicarbazide-HCl, 1.5% sodium acetate-3H_2O) was added; after incubation at room temperature for 1 h, the absorbance was measured at 250 nm with a UV-Vis spectrophotometer (ε = 10,200 cm^{-1} M^{-1}).

^{1}H and ^{13}C NMR Activity Assay of DkgM, ClxL, and ClxD
General reaction conditions to convert substrates to L-lyxonate contained 10 mM substrate, 0.1 mM NAD^+, with 1 µM of purified DkgM, ClxL, and ClxD in 50 mM sodium phosphate pH 7.2 in a final volume of 570 µL in a 1.7 mL microcentrifuge tube. After a 1 h incubation, 30 µL of DMSO-d_6 was added, the sample was moved to an NMR tube, and spectra were recorded. Initial reactions with 10 mM L-ascorbic acid required the addition of 0.1 mM ferrous ammonium sulfate to see 30% conversion to L-lyxonate. Full conversion is achieved with 10 mM L-dehydroascorbic acid. For full conversion of the labeled substrates 1-[13C]-L-ascorbic acid and 2-[13C]-L-ascorbic acid, each reaction contained one flake (<1 mg) of ascorbate oxidase.

Mass determination by LC-MS
Mass analysis of samples were analyzed by using the Q-Exactive MS system (Thermo Scientific, Bremen, Germany) in the Metabolomics Laboratory of Roy J. Carver Biotechnology Center, University of Illinois at Urbana-Champaign. The software Xcalibur 4.1.31.9 was used for data acquisition and analysis. The Dionex Ultimate 3000 series HPLC system (Thermo Scientific, Germering, Germany) used includes a degasser, an autosampler, and a binary pump. The LC separation was performed on a Phenomenex Kinetex C18 column (4.6 x 100 mm, 2.6 µm) with mobile phase A (H_2O with 0.1% formic acid) and mobile phase B (acetonitrile with 0.1% formic acid). The flow rate was 0.25 mL/min. The linear gradient was as follows: 0-3 min, 100% A; 20-30 min, 0% A; 30.5-36 min, 100% A. The autosampler was set at 15°C and the column was kept at room temperature. The injection volume was 20 µL. High-resolution mass spectra were acquired under both positive (sheath gas flow rate, 46; aux gas flow rate, 11; sweep gas flow rate, 2; spray voltage, 3.5 kV; capillary temp, 253 °C; Aux gas heater temp, 406 °C) and negative electrospray ionization (sheath gas flow rate, 46; aux gas flow rate, 11; sweep gas flow

rate, 2; spray voltage, -2.5 kV; capillary temp, 253 °C; Aux gas heater temp, 406 °C). The resolution of full scan mass spectrum was set at 70,000 with the scan range of m/z 70 ~ m/z 1,050, and the AGC target was 1E6 with the maximum injection time of 200 ms. For MS/MS scan, the mass spectrum resolution was set at 17,500, the AGC target was 5E4 with the maximum injection time of 50 ms, the loop count was 10, and the isolation window was 1.0 m/z with NCE of 25 eV and 40 eV.

^{1}H NMR, ^{13}C NMR, and mass spectral data for 2-carboxy-L-lyxonolactone and 2-carboxy-L-lyxonate.

2-carboxy-L-lyxonolactone: ^{1}H NMR (600 MHz, H$_2$O pH 7.2 5% DMSO-d_6) δ 4.69 (1H, ddd, J = 8.5, 7.3, 3.6 Hz, H4), 4.43 (1H, d, J = 7.3 Hz, H3), 3.93 (1H, dd, J = 12.2, 8.5 Hz, H5), 3.78 (1H, dd, J = 12.2, 3.6 Hz, H5) ppm; ^{13}C NMR (150 MHz, H$_2$O pH 7.2 5% DMSO-d_6) δ 178.6 (C1), 173.0 (COH<u>CO$_2$</u>$^-$), 84.0 (C2), 76.6 (C3,C4), 61.3 (C5). We cannot uniquely observe C3 and C4 peaks in any ^{13}C NMR spectra. ESI m/z: 191.02 [M-H]-.

2-carboxy-L-lyxonate: ^{1}H NMR (600 MHz, H$_2$O pH 7.2 5% DMSO-d_6) δ 4.16 (1H, d, J = 2.6 Hz, H3), 3.67 (1H, ddd, J = 7.2, 4.6, 2.6 Hz, H4), 3.45 (1H, dd, J = 11.6, 4.6 Hz, H5), 3.78 (1H, dd, J = 11.6, 7.2 Hz, H5) ppm; ^{13}C NMR (150 MHz, H$_2$O pH 7.2 5% DMSO-d_6) δ 177.7 (C1), 177.4 (C1'), 86.6 (C2), 73.7 (C3,C4), 65.0 (C5). We cannot uniquely observe C3 and C4 peaks in any ^{13}C NMR spectra. ^{13}C-labeled material does appear to separate these peaks, however. 1-[^{13}C]-2-carboxy-L-lyxonate causes splitting of C2 (86.5 ppm, J = 52.5 Hz) and separation between C3 and C4 (73.72 and 73.68 ppm). ESI m/z: 209.03 [M-H]-.

^{1}H NMR Activity Assay of LyxD, KdlD, and KgsD

Assays to verify conversion of L-lyxonate to α-ketoglutarate contained 5 mM L-lyxonate, 5 mM MgCl$_2$ in 20 mM sodium phosphate pH 7.2 in each assay. Assays either contained no enzyme or 1 µM enzymes LyxD, KdlD, and KgsD individually or in combination. Only in the case where all three enzymes were added was 0.5 mM NAD$^+$, 4.5 mM sodium pyruvate, and 0.016 mg/mL lactate dehydrogenase added to the reaction. These assays were performed in a final volume of 570 µL in a 1.7 mL microcentrifuge tube. After a 1 h incubation, 30 µL of DMSO-d_6 was added, the mixture was moved to an NMR tube, and the spectra were recorded.
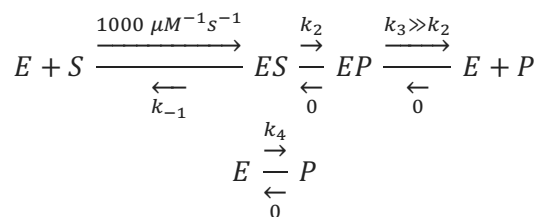
^{1}H NMR Activity Assay of DhaL

Due to the rapid hydrolysis of L-dehydroascorbate in buffer, the ^{1}H NMR assay for DhaL required immediate testing after the solution was prepared and monitoring by array. L-Dehydroascorbate was weighed in a test tube (1.7 mg) and dissolved in 600 µL of 25 mM sodium phosphate pH 7.2, 50% D$_2$O (L-dehydroascorbate concentration of 16 mM), and immediately added to an NMR tube for a ^{1}H NMR spectrum to be recorded. To this solution, 10 µL of 90 µM purified DhaL in 50 mM sodium phosphate pH 7.6 was added (final enzyme concentration of 1.5 µM). A new ^{1}H NMR spectrum was taken every two minutes, until reaction was completed ten minutes after enzyme addition.

Kinetic Analysis of DhaL, DkgM, and ClxL

The enzymatic hydrolysis of either L-dehydroascorbate or 2-carboxy-L-lyxonolactone was monitored by detecting the protons released from the carboxylate product using the pH indicator bromothymol blue.[5] The enzyme DhaL was exchanged into 2.5 mM MOPS pH 7.2, 0.2 M NaCl, while enzymes DkgM, and ClxL were exchanged into 2.5 mM sodium phosphate pH 7.2, 0.2 M NaCl before use in kinetic analysis.

Full reaction progress curves were monitored for the reaction of DhaL with L-dehydroascorbate and compared to the nonenzymatic rate of hydrolysis. Enzymatic tests have 90 nM enzyme, while varying L-dehydroascorbate from 0.1-1.0 mM (stock concentration 10 mM in 10% DMSO). Reactions are performed in 200 µL total reactions in 2.5 mM MOPS pH 7.2, 0.2 M NaCl, 0.1 mM bromothymol blue (made from a stock solution of 200 mM bromothymol blue in DMSO). Rates of conversion were monitored by aliquoting enzyme into a 96-well microplate, preparing the L-dehydroascorbate solution, and quickly adding substrate solution to the microplate to monitor enzymatic and nonenzymatic rate simultaneously over 1 hr. The appearance of product was measured by following the absorbance at

616 nm in a plate reader at 25 °C. The data was imported to KinTek Explorer Pro where the following simplified model was fit:

$$E + S \xrightleftharpoons[k_{-1}]{1000\ \mu M^{-1}s^{-1}} ES \xrightleftharpoons[0]{k_2} EP \xrightleftharpoons[0]{k_3 \gg k_2} E + P$$

$$E \xrightleftharpoons[0]{k_4} P$$

The simple model assumes diffusion-controlled substrate binding to the enzyme, with an irreversible chemistry step, fast product release and no product rebinding. Globally fitting the enzymatic and nonenzymatic data as two separate experiments, while including both a constant factor and an offset factor to convert the raw absorbance value into a change in concentration and allow a change to the initial absorbance, respectively, provided a reliable fit. The determined $k_{cat} = k_2$ and the $K_m = k_{-1}/(1000\ \mu M^{-1}s^{-1})$.[6]

Full reaction progress curves were monitored for the reactions of DkgM and ClxL by varying 2,3-diketo-L-gulonate (DKG) as substrate for DkgM, and monitoring proton release by the activity of the amidohydrolase ClxL, by coupling these enzyme activities together. A solution of 10 mM DKG is generated by incubating 10 mM L-dehydroascorbate in 20 mM dibasic sodium phosphate for 2 hr (conversion was verified by ^{1}H NMR). The indicator dye bromothymol blue (200 mM in DMSO) was added to this DKG solution to obtain a final concentration of 0.1 mM, and the pH adjusted to 7.2. This substrate solution was mixed with 20 mM sodium phosphate pH 7.2 and 0.1 mM bromothymol blue to vary substrate concentration from 1.0 to 10 mM DKG, and then diluted with 0.2 M NaCl, 0.1 mM bromothymol blue to make final assay concentration 2.0 mM sodium phosphate pH 7.2, 0.18 M NaCl, 0.1 mM bromothymol blue, with varying DKG concentrations from 0.1-1.0. mM DKG. To test for the kinetics with DkgM, these solutions were then added to 0.1 µM DkgM and 3.0 µM ClxL (final concentrations) previously aliquoted into a 96-well microplate and compared to nonenzymatic rates. ClxL was verified to not be rate-limiting in this assay setup.

To determine the kinetics for ClxL, DkgM was first added to the 10 mM DKG stock solution to make 2-carboxy-L-lyxonolactone *in situ*. By ^{1}H NMR, 160 nM DkgM fully processed 10 mM substrate in 22 min, while the product is stable during the full hour monitored. In a similar process as described above, 10 mM DKG solution is made, the pH is adjusted to 7.2, and DkgM is added to a final concentration of 160 nM. DkgM is added, and after a 25 min incubation, the kinetic assay is set up as described above, using 0.065 µM Q0K1W9 to measure enzymatic rates and compared to nonenzymatic rates.

In both cases these assays were monitored for 30 min in a 96-well microplate, and the absorbance at 616 nm was measured using a plate reader at 25 °C. The raw data was fit using KinTek Explorer Pro using the same method described for DhaL.

Enzymatic Synthesis and Purification of 2-carboxy-L-lyxonate
The intermediate 2-carboxy-L-lyxonate was generated from 100 mg L-dehydroascorbate in 20 mL 50 mM sodium pyruvate pH 7.2, with 65 nM DkgM and 6.5 nM Q0K1W9. After an overnight incubation, 0.32 g of magnesium acetate monohydrate (75 mM) is added, and the pH is adjusted to 8 using 1 M NaOH. The mixture is incubated at 65 °C for 15 min, and the mixture is spun for 15 min at 5,000 × g. (These steps cause magnesium phosphate and enzymes to precipitate). The pellet is disposed. The supernatant is added to 10 mL of Dowex 1x2 chloride form 100-200 mesh equilibrated with water. The resin is washed with 100 mL of water until eluent is acidic, and then eluted with 40 mL of 1 M potassium acetate. This solvent is removed through evaporation, and the resulting solids are rinsed with ethanol to remove excess potassium acetate. The solvent is removed through evaporation, and any remaining solvent or volatile solids are removed by lyophilization.

Kinetic Analysis of ClxD

The decarboxylation of 2-carboxy-L-lyxonate was measured using a coupled assay with phosphoenolpyruvate carboxylase (PEPC) and malate dehydrogenase (MDH) to detect CO_2. (Note: The assay requires complete removal of dissolved CO_2, so all components must be made fresh and buffers purged of nitrogen through boiling, sonication, and cooling under a flow of N_2 gas for 1 hr. A separate problem to address is to verify the enzymatically generated and purified substrate to have the correct concentration by integrating proton signals in ^{1}H NMR with an internal standard.)

Assay conditions contained 1.0 mM phosphoenolpyruvate, 0.6 mM NADH, 5 mM $MgCl_2$, 5 U PEPC, 5 U MDH, and 2 µM ClxD (pre-incubated with 0.1 mM NAD^+) in 100 mM Tris-HCl pH 7.5. Initial rates were measured at 25 °C for 3 min and fit to a zero-order equation. The rate of disappearance of NADH was measured by following the absorbance at 340 nm (ε = 6220 M^{-1} cm^{-1}) in a plate reader. Assays were performed in triplicate, averaged, and the rates corrected for the background rate of NADH oxidation in the absence of enzyme. These corrected rates were plotted versus initial substrate concentration and fit to determine k_{cat} and K_m through nonlinear regression analysis performed using Mathematica.

^{1}H NMR Full Kinetic Time Course of ClxD Reaction

To monitor the conversion of 2-carboxy-L-lyxonate to L-lyxonate by ^{1}H NMR, an initial spectrum was taken of a sample containing 570 µL of 10 mM 2-carboxy-L-lyxonate (the same stock used for kinetic analysis by UV-Vis) mixed with 30 µL DMSO-d_6. Then 20 µL of ClxD (180 µM stock concentration, 6 µM final concentration) and 0.5 µL NAD^+ (8 mM stock concentration, 6.5 µM final concentration) was added, and ^{1}H NMR taken every 3 min after enzyme addition. The relative conversion of substrate to products was determined by comparing the integrations of the C2 proton (δ 3.94-3.90 ppm) of the product L-lyxonate to the residual solvent peak of DMSO-d_6 (δ 2.53-2.48 ppm). The reaction had mostly finished within 24 min, however a final ^{1}H NMR was taken 18 h later to measure final integrations. The percent conversion to products was converted to product concentration and plotted over time. This full-time reaction course was fit using KinTek Explorer Pro to provide a lower boundary to k_{cat}.

Stopped-Flow Analysis of ClxD Reaction

To test for the transient formation of NADH, a stopped-flow experiment was performed using an Applied Photophysics SX20 stopped-flow spectrophotometer equipped with a circulating water bath. In this experiment, one syringe contained 1.2 mM ClxD and 2 mM NAD, the second syringe contained 2 mM 2-carboxy-L-lyxonate, both in 100 mM sodium phosphate pH 6.8 incubated at 4 °C. Upon mixing, the absorbance changes between 200 and 800 nm were monitored over 1 s, measuring 1000 points. Control reactions were performed by replacing enzyme or substrate with buffer only.

Enzymatic and Nonenzymatic $^{13}CO_2$ Incorporation during Conversion of DKG into Clx

To test for exogenous CO_2 incorporation in the nonenzymatic conversion of 2,3-diketo-L-gulonate to 2-carboxy-L-lyxonate, L-dehydroascorbate was incubated with ^{13}C-labeled sodium bicarbonate under alkaline conditions. Unlabeled carbon dioxide and bicarbonate was removed by sonicating and sparging all buffers and solutions before dissolving sodium bicarbonate into solution and left to react under N_2 headspace. Exact mass of the samples were determined by LC-MS (described above), and percentage of ^{13}C in the Clx product was determined through integrations of extracted ion chromatograms in the program Thermo Xcalibur 4.1.31.9.

To a 4 mL aliquot of 125 mM NaPO4 pH 7.4, 50 µL of 5 M HCl was added, followed by 420 µL of 6 M NaOH (note: this volume of acid and base were empirically determined using unlabeled bicarbonate under atmospheric conditions to result in a final pH of 12.0). This buffer and an aliquot of water was sonicated and left under a stream of N_2 gas to remove atmospheric carbonate and carbon dioxide.

In a 1.5 mL microcentrifuge tube, 12.5 mg of $NaHCO_3$ or $NaH^{13}CO_3$ was dissolved into 450 µL of the sparged buffer under a constant stream of nitrogen. To 14.1 mg L-dehydroascorbate, 816 µL of sparged water was added, quickly mixed, and 50 µL of this mixture was added to the two tubes. Final reaction conditions result in 0.5 mL of 100 mM sodium phosphate pH 12.0, 300 mM sodium bicarbonate ($NaHCO_3$

in control reaction, NaH^{13}CO$_3$ in test reaction), and 10 mM L-dehydroascorbate. Triplicate reactions were left at room temperature overnight (18 h incubation) under headspace of N$_2$ gas in 50 mL centrifuge tubes sealed with electrical tape.

To test for exogenous CO$_2$ incorporation in the DkgM-catalyzed conversion of 2,3-diketo-L-gulonate to 2-carboxy-L-lyxonate, a similar experiment was used as above. Instead of 6 M NaOH, 420 µL of water was added, so when the sodium bicarbonate is dissolved in this solution, the final pH was 7.0. 10 µL of 20 µM DkgM was diluted to 100 µL using the sparged sodium phosphate buffer, and 10 µL of this enzyme was added to the two separate hungate tubes. Final reaction conditions result in 1 mL of 100 mM sodium phosphate pH 7.0, 300 mM sodium bicarbonate (NaHCO$_3$ in control reaction, NaH^{13}CO$_3$ in test reaction), 10 mM L-dehydroascorbate, 20 nM DkgM. Triplicate reactions were left at room temperature overnight (18 h incubation) under headspace of N$_2$ gas in 50 mL centrifuge tubes sealed with electrical tape.

Description of methodology to generate SSN images
The EFI-EST web tool (http://efi.igb.illinois.edu/efi-est/) was used to generate sequence similarity networks (SSNs) of enzymes encoded by the candidate genes. All networks were generated using UniProt: 2019-04 / InterPro: 74.

The SSN of Q0K7D4 (DhaL, dehydroascorbate lactonase, representing module 1) was generated through analysis of PF08450, the "SMP-30/Gluconolactonase/LRE-like region (SGL)" family using the UniRef90 database. These 40,475 sequences (21,264 metanodes) were first filtered for full-length proteins by applying a minimum amino acid length of 240 (resulting in 19,833 metanodes). Initial fractionation was performed using an alignment score of 86 (~ID 50%) (Figure S3A). The cluster containing Q0K7D4 was further separated by increasing the alignment score to 120. The resulting network may represent different phylogeny or metabolic pathways, all including dehydroascorbate lactonase, as many clusters display co-localization with the enzymes involved in the known *E. coli* metabolic pathway for ascorbate (Figure S3B). To identify the organisms that include module 1 of the *R. eutropha* pathway, those that were co-localized with the 2,3-diketo-L-gulonate mutase were identified (Figure S3C).

The SSN of Q0K1W7 (DkgM, 2,3-diketo-L-gulonate mutase, representing module 2) was generated through a BLAST search of the query sequence (Q0K1W7, not recognized as part of a Pfam). This search retrieved 1,759 sequences. These sequences were first filtered for full-length proteins by applying a minimum amino acid length of 250 and filtered to removed large, multidomain proteins by applying a maximum amino acid length of 800 (resulting in 1,637 nodes). Initial fractionation was performed using an alignment score of 60 (~ID 45%) (Figure S4A). The cluster containing Q0K1W7 was further separated by increasing the alignment score to 88 and analyzed for co-occurrence with other L-ascorbate metabolic genes (Figure S4B).

The SSN of Q0K4Q7 (ClxD, 2-carboxy-L-lyxonate decarboxylase, representing module 3) was generated through analysis of PF04166, the "Pyridoxal phosphate biosynthetic protein PdxA (PdxA)" family using the UniRef90 database. These 23,571 sequences (10,639 metanodes) were first filtered for full-length proteins by applying a minimum amino acid length of 275 (resulting in 9,751 metanodes). Initial fractionation was performed using an alignment score of 85 (~ID 50%) (Figure S5A). The cluster containing Q0K1W7 was further separated by increasing the alignment score to 105 and analyzed for co-occurrence with other L-ascorbate metabolic genes (Figure S5B).

See supplementary Excel file "List of UniProt IDs" for homologues of Q0K7D4 (DhaL, dehydroascorbate lactonase, representing module 1), Q0K1W7 (DkgM, 2,3-diketo-L-gulonate mutase, representing module 2), and Q0K4Q7 (ClxD, 2-carboxy-L-lyxonate decarboxylase, representing module 3).
Supplementary Tables

Table S1. Top BLAST hits in the *R. eutropha* genome to the Ula or Sga enzymes from *E. coli*

E. coli proteins	Top BLAST hit from *R. eutropha* H16

	NCBI ID	UniProt ID	Enzyme Name	NCBI ID	UniProt ID	Query Coverage	ID	Similarity	E value
ulaA	NP_418614.4	P39301	Ascorbate-specific PTS system EIIC component	no significant similarity found					
ulaD	NP_418038.1	P37678	3-keto-L-gulonate-6-phosphate decarboxylase	no significant similarity found					
ulaE	NP_418039.2	P37679	L-ribulose-5-phosphate 3-epimerase	no significant similarity found					
ulaF	NP_414603.1	P08203	L-ribulose-5-phosphate 4-epimerase	QCC04595.1	Q0JZP2	78%	24%	42%	3E-08
ulaG	NP_418613.2	P39300	L-ascorbate-6-phosphate lactonase	QCC00247.1	Q0KCC4	11%	36%	50%	0.68
yiaK	NP_418032.1	P37672	2,3-diketo-L-gulonate reductase	QCC03061.1	Q0K4E0	86%	28%	50%	7E-31
yiaP	NP_418037.1	P37677	L-xylulose/3-keto-L-gulonate kinase	QCC01756.1	R7XD08	5%	58%	65%	2

Table S2. Gene Products Involved in the Catabolic Pathway of L-ascorbate in *R. eutropha*

Locus Tag	Co-Occurrence with H16_B0216[a]	Protein Name	Family ID	UniProt ID	Transcript Fold Upregulation[b]	Proposed gene name
H16_A3010	<20%	*putative L-ascorbate oxidoreductase*	PF03188	Q0K7D6	894	*laaO*
H16_A3011	<20%	*putative transporter*	PF02447	Q0K7D5	597	
H16_A3012	<20%	L-dehydroascorbate lactonase	PF08450	Q0K7D4	360	*dhaL*
H16_B1217	147/550	2,3-diketo-L-gulonate mutase	IPR015943, IPR011048	Q0K1W7	590	*dkgM*
H16_B1218	300/550	*putative transporter*	PF07690	Q0K1W6	504	
H16_B1219	273/550	2-carboxy-L-lyxonolactonase	PF04909	Q0K1W5	383	*clxL*
H16_B0212	275/550	α-ketoglutarate semialdehyde dehydrogenase	PF00171	Q0K4R1	290	*kgsD*
H16_B0213	319/550[c]	2-keto-3-deoxy-L-lyxonate dehydratase	PF00701	Q0K4R0	305	*kdlD*
H16_B0215	300/550	*putative transporter*	PF03401	Q0K4Q8	450	
H16_B0216	N/A	2-carboxy-L-lyxonate decarboxylase	PF04166	Q0K4Q7	308	*clxD*
H16_B0217	484/550	L-lyxonate dehydratase	PF02746, PF13378	Q0K4Q6	888	*lyxD*

a. Co-occurrence ratio given from summation of appropriate clusters shown in Figure S5B, and is counted if a gene of the given Pfam is found in ± 10 ORFs of the *h16_b0216* ortholog. Not defined if below 20% co-occurrence. Ratio counts number of unique UniProt IDs.
b. Upregulation when *R. eutropha* is grown on L-ascorbate compared to growth on D-fructose
c. This counts the number of ORFs defined by PF00701. This gene may be replaced by a non-ortholog (member of the fumarylacetoacetate hydrolase superfamily) as found in *Pseudomonas aeruginosa* PAO1, and is found co-occurrent in 123/550 sequences

Table S3. Percent identity and similarity of *R. eutropha* and *Pseudomonas aeruginosa* or *Labrenzia aggregata* catabolic genes for L-lyxonate

R. eutropha UniProt	Compared to organism	UniProt	% ID	% similarity
Q0K4Q6	*Pseudomonas aeruginosa*	Q9I1Q2	84	91
Q0K4R1	*Pseudomonas aeruginosa*	Q9I1Q0	51	63
Q0K4R0	*Labrenzia aggregata*	A0NP47	54	68

Table S4. Strains used in this study

| Strain name	Relevant Characteristics	Source Strain	Reference
NEB5α		*Escherichia coli*	
Rosetta2 (DE3)		*Escherichia coli*	
S17		*Escherichia coli*	
DH5α		*Escherichia coli*	
R. eutrophaH16	Wild Type	*Ralstonia eutropha* H16	DSM-428
ReΔ*B1219*	795 bp of 951 bp of *h16_B1218* deleted	*Ralstonia eutropha* H16	This study
ReΔ*A3012*	858 bp of 909 bp of *h16_A3012* deleted	*Ralstonia eutropha* H16	This study
ReΔ*B1218*	1190 bp of 1388 bp of *h16_B1218* deleted	*Ralstonia eutropha* H16	This study
ReΔ*A3010*	816bp of 861bp of *h16_A3010* deleted	*Ralstonia eutropha* H16	This study
ReΔ*B1217*	867bp of 945bp of *h16_B1217* deleted	*Ralstonia eutropha* H16	This study
ReΔ*B0215*	861bp of 969bp of *h16_B0215* deleted	*Ralstonia eutropha* H16	This study
ReΔ*B0213*	839bp of 933bp of *h16_B0213* deleted	*Ralstonia eutropha* H16	This study
ReΔ*B0216*	885bp of 1017bp of *h16_B0216* deleted	*Ralstonia eutropha* H16	This study
ReΔ*A3011*	1311bp of 1374bp of *h16_A3011* deleted	*Ralstonia eutropha* H16	This study
ReΔ*B0217*	1086bp of 1176 bp of *h16_B0217* deleted	*Ralstonia eutropha* H16	This study

Table S5. Primers and plasmid used in this study

| Primer Sequences	Purpose	Locus Tag UniProt ID	Plasmid
Heterologous protein production constructs			
ctggtgccgcgcggcagccatATGCCACCTGCGCTTCCC tcgggctttgttagcagccggatcCTAATCCTTGTGTTCAGCCGGC	Amplify *h16_A3010 to clone into pET15b*	H16_A3010 Q0K7D6	Q0K7D6 pET15b
ctggtgccgcgcggcagccatATGGATACAGTCCGGATATTCG tcgggctttgttagcagccggatccTCACGTCAAGCGCTGACC	Amplify *h16_A3012 to clone into pET15b*	H16_A3012 Q0K7D4	Q0K7D4 pET15b
ctggtgccgcgcggcagccatATGGAAAGCCAATGGACGG tcgggctttgttagcagccggatcCTACCGCGTCGGCAAAGC	Amplify *h16_B1217 to clone into pET15b*	H16_B1217 Q0K1W7	Q0K1W7 pET15b
ctggtgccgcgcggcagccatATGAGCAGCGTAACAACTGCC tcgggctttgttagcagccggatcCTAGGCCAGCTCGGACGG	Amplify *h16_B1219 to clone into pET15b*	H16_B1219 Q0K1W5	Q0K1W5 pET15b
ctggtgccgcgcggcagccatATGACAATCTCAGGCGAACTCC tcgggctttgttagcagccggatccTCAGCCGGGCATCCCTTG	Amplify *h16_B0212 to clone into pET15b*	H16_B0212 Q0K4R1	Q0K4R1 pET15b
ctggtgccgcgcggcagccatATGACCCGCACCCCATCCC tcgggctttgttagcagccggatccTCAGCGGGCCCAGCGCAG	Amplify *h16_B0213 to clone into pET15b*	H16_B0213 Q0K4R0	Q0K4R0 pET15b
ctggtgccgcgcggcagccatATGAATTCCCGTCCAAGAATCGCCATG tcgggctttgttagcagccggatcCTAGGCTGTGGCGCGCCG	Amplify *h16_B0216 to clone into pET15b*	H16_B0216 Q0K4Q7	Q0K4Q7 pET15b
ctggtgccgcgcggcagccatATGAAGATCACCAACGTCC tcgggctttgttagcagccggatccTCAGCCGATGATGTCGAAC	Amplify *h16_B0217 to clone into pET15b*	H16_B0217 Q0K4Q6	Q0K4Q6 pET15b
Mutation constructs			
CTTGCATGCCTGCAGGTCGACTCTAGAGCTGACCATGGTCGGCAACTGGTTTC ATAGAACCTGGCTTCGTCCTGCAGCCAGGGATAGC	Amplify upstream fragment for deletion of *h16_B1219*	H16_B1219 Q0K1W5	pMC252
CTGCAGGACGAAGCCAGGTTCTATCGGATCAATGTTCCAAG GAATTCGAGCTCGGTACCCGGGGATCCGGTAATGGCTCCAATTCAGTCATCGCCTG	Amplify downstream fragment for deletion of *h16_B1219*	H16_B1219 Q0K1W5	pMC252
TTCGAGCTCGGTACCCGGGGATCCGCGTCGGCATTCCGGTGTTCTTTG GCGCTGACCAAGGCGCTCATCGAATATCCGGACTGTATCC	Amplify upstream fragment for deletion of *h16_A3012*	H16_A3012 Q0K7D4	pPK001
TTCGATGAGCGCCTTGGTCAGCGCTTGACGTGAG GCATGCCTGCAGGTCGACTCTAGATGCCTGTCATGGTCATGAGACACTAGC	Amplify downstream fragment for deletion of *h16_A3012*	H16_A3012 Q0K7D4	pPK001
CTTGCATGCCTGCAGGTCGACTCTAGAAGTTGCCTGACTATCCGCATGAATTCG GTAGACACCGGCACCGGTGAGTGGTGTCGCATC	Amplify upstream fragment for deletion of *h16_B1218*	H16_B1218 Q0K1W6	pYN003
CCACTCACCGGTGCCGGTGTCTACCTGCTGGTC GAATTCGAGCTCGGTACCCGGGGATCCCGGCCTTGGAACATTGATCCGATAGAAC	Amplify downstream fragment for deletion of *h16_B1218*	H16_B1218 Q0K1W6	pYN003
TTCGAGCTCGGTACCCGGGGATCCGTTCTCGCTGTTCTCGCTGATGGATACG GTGTTCAGCCGGAAGCGCAGGTGGCATTTCCGATCTC	Amplify upstream fragment for deletion of *h16_A3010*	H16_A3010 Q0K7D6	pBW001

CCACCTGCGCTTCCGGCTGAACACAAGGATTAGACGTGG GCATGCCTGCAGGTCGACTCTAGAAGCAACAGCGCGACGTATGGGATG	Amplify downstream fragment for deletion of *h16_A3010*	H16_A3010 Q0K7D6	pBW001
GCATGCCTGCAGGTCGACTCTAGAAGCAACAGCGCGACGTATGGGATG GGCAAGACCGTCGCTGAAGCTATGGCCGAATTTCTCCAC	Amplify upstream fragment for deletion of *h16_B1217*	H16_B1217 Q0K1W67	pMC251
CATAGCTTCAGCGACGGTCTTGCCATCCTGGCTTTG GAATTCGAGCTCGGTACCCGGGGATCCCGGCCAGACCACGAAGTCCTTG	Amplify downstream fragment for deletion of *h16_B1217*	H16_B1217 Q0K1W67	pMC251
CTTGCATGCCTGCAGGTCGACTCTAGAGGAGCTGGAAGGCATGCTGGAAG CTTGCCATAGCGCGCCCAGGCATTGCCCGTTAC	Amplify upstream fragment for deletion of *h16_B0215*	H16_B0215 Q0K4Q8	pYN004
AATGCCTGGGCGCGCTATGGCAAGCTGATCGCTGAACTG GAATTCGAGCTCGGTACCCGGGGATCCGCCCTGCTGCGTGATGTCGAAC	Amplify downstream fragment for deletion of *h16_B0215*	H16_B0215 Q0K4Q8	pYN004
CTTGCATGCCTGCAGGTCGACTCTAGACGCAGTGCGCGGCAATGCCTTCAG CAGCCCTTCGCGGAATACGCCGCGGTAGACGGTG	Amplify upstream fragment for deletion of *h16_B0213*	H16_B0213 Q0K4R0	pMC248
GAATTCGAGCTCGGTACCCGGGGATCCCGGCGCAATAGGCACGATGGATG CGCGGCGTATTCCGCGAAGGGCTGCTGAAGATTGC	Amplify downstream fragment for deletion of *h16_B0213*	H16_B0213 Q0K4R0	pMC248
CTTGCATGCCTGCAGGTCGACTCTAGAGACGGAGACAGCAATGAAGACATGGATCG GTCGAACGCGGTCATGGCGATTCTTGGACGGGAATTCATTG	Amplify upstream fragment for deletion of *h16_B0216*	H16_B0216 Q0K4Z2	pMC249
AGAATCGCCATGACCGCGTTCGACATCACGCAG GAATTCGAGCTCGGTACCCGGGGATCCTCCTTGAAGCCGTAGGAGGTGAATTCATGTTC	Amplify downstream fragment for deletion of *h16_B0216*	H16_B0216 Q0K4Z2	pMC249
GCATGCCTGCAGGTCGACTCTAGACCGCTATCCACCCTCTGTCCCATTC GATCAGGCCAAGCGCACCGCCGAATATCAGTATTGCC	Amplify upstream fragment for deletion of *h16_A3011*	H16_A3011 Q0K7D5	pRJ001
TTCGGCGGTGCGCTTGGCCTGATCCTCTTGCTGTGG GAATTCGAGCTCGGTACCCGGGGATCCGCTGGAGTTCGTCGAAACGCGCTAAG	Amplify downstream fragment for deletion of *h16_A3011*	H16_A3011 Q0K7D5	pRJ001
CTTGCATGCCTGCAGGTCGACTCTAGAGCCGAGATCCTGTTGATCGCCGAC GAAGTACTCCTCCACGGTCTTGCCCTTCCATTCAAAGACAC	Amplify upstream fragment for deletion of*h16_B0217*	H16_B0217 Q0K4Q6	pMC250
GGCAAGACCGTGGAGGAGTACTTCAGCCAGTTCGACATCATC GAATTCGAGCTCGGTACCCGGGGATCCGGAAATCATCCTCGAACGCCTCGGATTC	Amplify downstream fragment for deletion of *h16_B0217*	H16_B0217 Q0K4Q6	pMC250

Complementation Constructs			
CTCCACCGCGGTGGCGGCCGCTCTAGACAGGGTACGCGCTCTTTGCGTGTG TACGCTGCTCATTCTGTCTCCTTGTGATTCGCACGCC	Amplify promoter for complementation of ReΔB1219	H16_B1219 Q0K1W5	pYN009
CAAGGAGACAGAATGAGCAGCGTAACAACTGCCGCGCTG ATCGAATTCCTGCAGCCCGGGGGATCCGCCGCTGGTTCTAGGCCAGCTC	Amplify coding region for complementation of ReΔB1219	H16_B1219 Q0K1W5	pYN009
CTCCACCGCGGTGGCGGCCGCTCTAGAAATGGCCGAAGGCATTGGGACG ATCGAATTCCTGCAGCCCGGGGGATCCTCGCCTGAGATTGTCATGCCTTGTCC	Amplify promoter and coding region for complementation of ReΔB0213	H16_B0213 Q0K4R0	pKB001
CACCGCGGTGGCGGCCGCTCTAGAGCAAGGCCGACAAGAATGTCGTGAAGAAATAG GACTGTATCCATTTCCGATCTCCTGATGCGCGGAGAATTCCTT	Amplify promoter for complementation of ReΔA3012	H16_A3012 Q0K7D4	pYN002
AGGAGATCGGAAATGGATACAGTCCGGATATTCGATGAGCG GAATTCCTGCAGCCCGGGGGATCCTGGAGTTCGTCGAAACGCGCTAAGG	Amplify coding region for complementation of ReΔA3012	H16_A3012 Q0K7D4	pYN002
CTCCACCGCGGTGGCGGCCGCTCTAGACAGTCGCGGCAGCAGACTTTTGG GGTGATCTTCATTGCTGTCTCCGTCGTTTTGCTGTC	Amplify promoter region for complementation of ReΔB0217	H16_B0217 Q0K4Q6	pRJ003
ACGGAGACAGCAATGAAGATCACCAACGTCCGCGCC ATCGAATTCCTGCAGCCCGGGGGATCCCGCGCATTGTCGTGAAACATGGC	Amplify coding region for complementation of Re Δ B0217	H16_B0217 Q0K4Q6	pRJ003
CTCCACCGCGGTGGCGGCCGCTCTAGACGCAATGGCCGAAGGCATTGGG TGAGATTGTCATGGACTCCTCCGGCTGCTTGTGAATTGG	Amplify promoter region for complementation of Re Δ B0212	H16_B0212 Q0K4R1	pMJ007
CCGGAGGAGTCCATGACAATCTCAGGCGAACTCCTGATCGG ATCGAATTCCTGCAGCCCGGGGGATCCTCAGCCGGGCATCCCTTGCAGCTTG	Amplify coding region for complementation of Re Δ B0212	H16_B0212 Q0K4R1	pMJ007
CTCCACCGCGGTGGCGGCCGCTCTAGACAGTCGCGGCAGCAGACTTTTGG ACGGGAATTCATTGCTGTCTCCGTCGTTTTGCTGTCC	Amplify promoter for complementation of Re Δ B0216	H16_B0216 Q0K4Z2	pYN010
ACGGAGACAGCAATGAATTCCCGTCCAAGAATCGCCATGGTG GAATTCCTGCAGCCCGGGGGATCCGTGTGGTGAAGGTGGTGGCTAGG	Amplify coding region for complementation of Re Δ B0216	H16_B0216 Q0K4Z2	pYN010

|			
CTCCACCGCGGTGGCGGCCGCTCTAGACAGGGTACGCGCTCTTTGCGTGTG ATCGAATTCCTGCAGCCCGGGGGATCCCTCTGTCTCCGTATGGATTTCCGGGTATGG	Amplify coding region and promoter for complementation of Re ΔB1217	H16_B1217 Q0K1W6	pMJ002
CACCGCGGTGGCGGCCGCTCTAGAGCAAGGCCGACAAGAATGTCGTGAAGAAATAG GAATTCCTGCAGCCCGGGGGATCCCCGCCGAATATCAGTATTGCCACGTC	Amplify coding region and promoter for complementation of Re ΔA3010	H16_A3010 Q0K1W6	pMJ001

Supplementary Figures
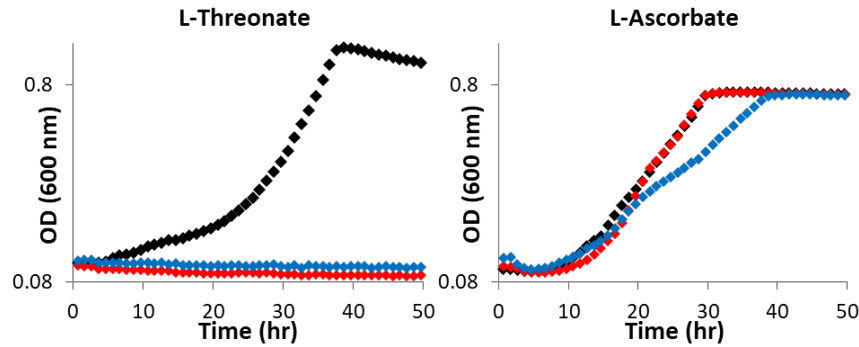
Figure S1. Growth of Ralstonia eutropha with L-ascorbate does not require L-threonate metabolic genes. Growth curves of R. eutropha wild type (black) and mutants lacking h16_A1561 (red) or h16_A1562 (blue), genes that encode enzymes in the L-threonate catabolic pathway in *R. eutropha.*[7]
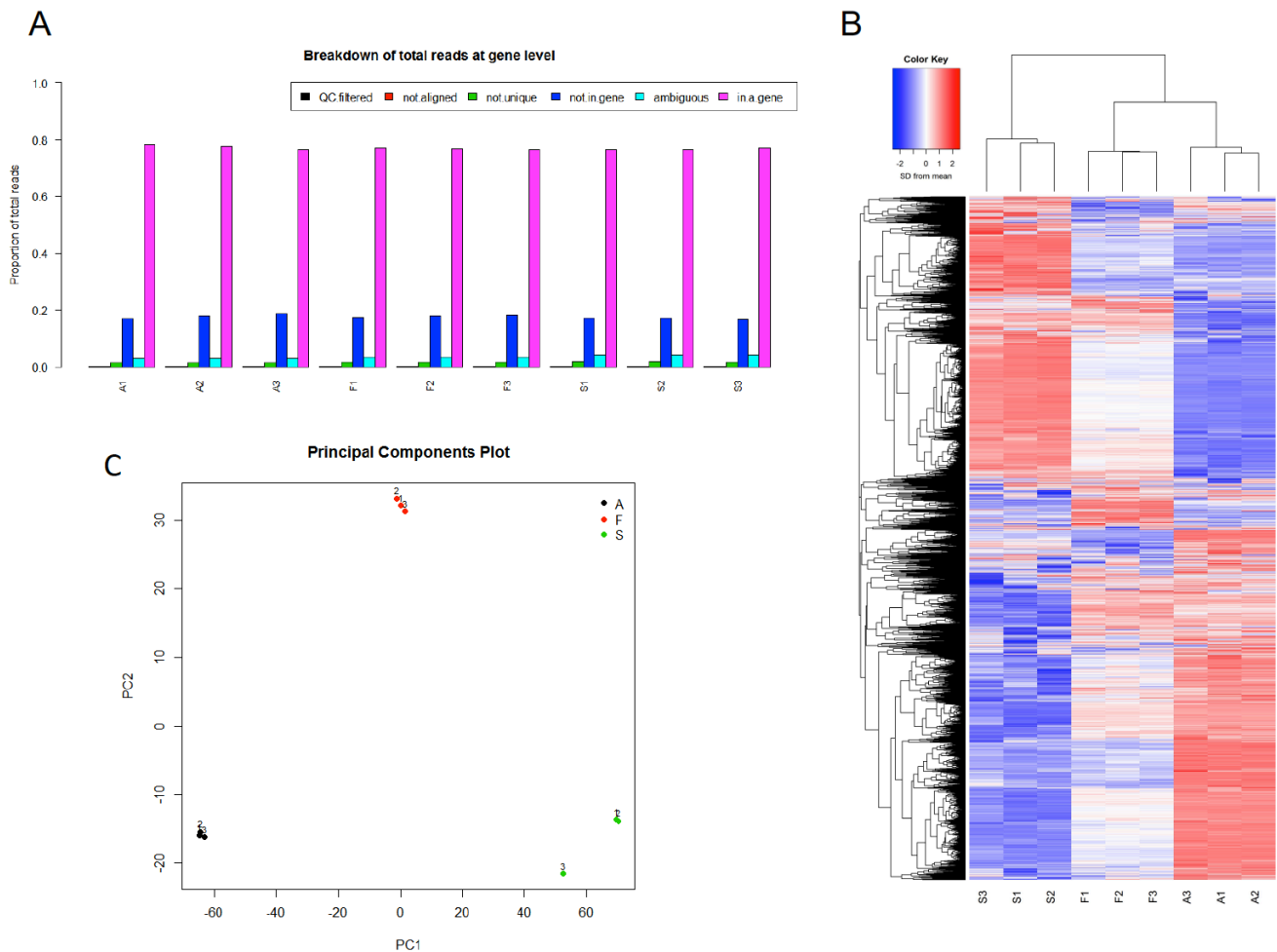
Figure S2. RNA-seq was used to quantify whole cell transcripts from cells grown with L-ascorbate, succinate, or D-fructose. Out of the 6,634 genes, 6,462 were detected (>= 10 reads) in at least 3 samples. S = succinate, F = D-fructose, A = L-ascorbate. Each carbon source was tested across three samples. A) Breakdown of total reads at the gene level. B) Hierarchical clustering of RNA reads visualized by a heatmap. C) Principal component plot of all 9 samples. See supplementary Excel file "List of Upregulated Genes" to see the full list of genes that were found upregulated when R. eutropha is grown on L-ascorbate as the sole carbon source compared to growth on D-fructose and succinate.
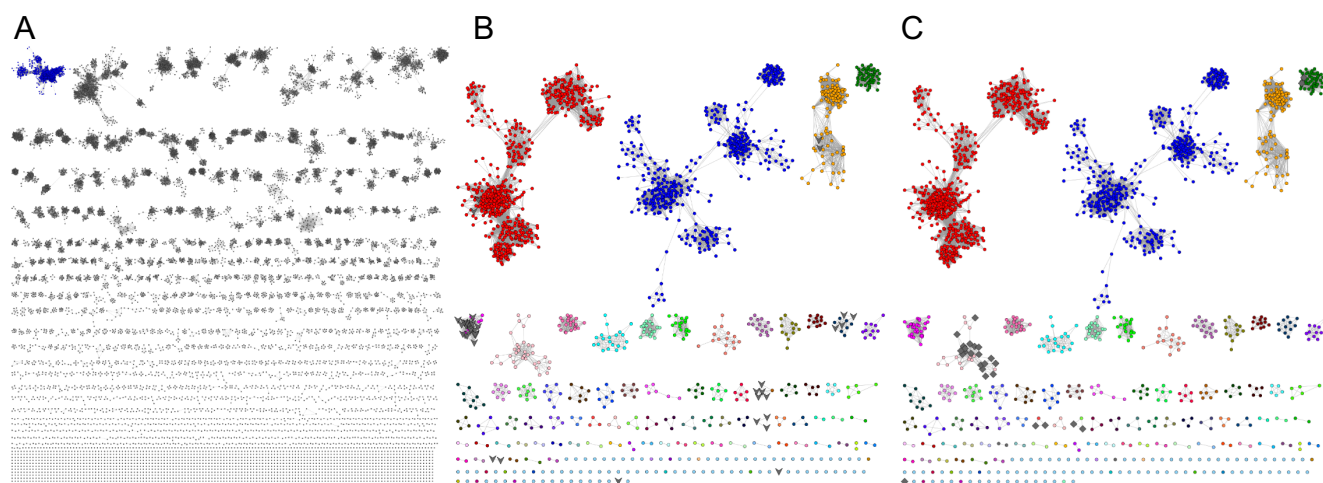
Figure S3. SSN analysis of PF08450 to find Q0K7D4 (DhaL) homologs. A) UniRef90 network of PF08450, minimum length 240 amino acids, displayed using an alignment score of 86. Our sequence of interest (Q0K7D4) is in cluster 1 (colored blue). B) SSN of cluster 1 from panel A, displayed using an alignment score of 120. Individual clusters are given a unique color. Sequences that are genetically encoded within ten orfs from PF00215 (OMPdecase, 3-keto-L-gulonate-6-phosphate decarboxylase) are shown as gray "V"s. C) SSN of cluster 1 from panel A, displayed using an alignment score of 120. Individual clusters are given a unique color. Sequences that are genetically encoded within ten orfs from 2,3-diketo-L-gulonate mutase are shown as gray diamonds.
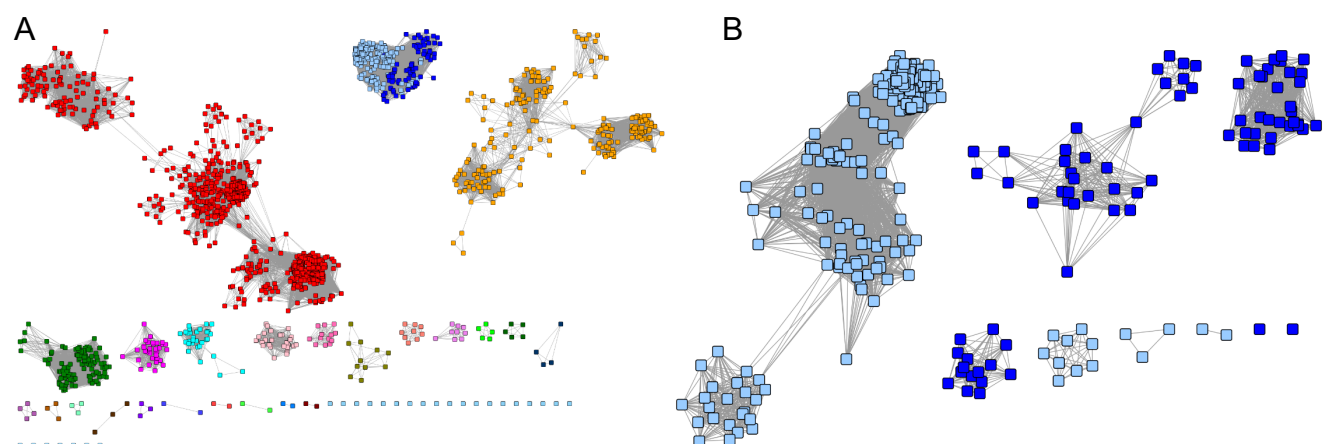
Figure S4. SSN analysis of Q0K1W7 (DkgM) homologs. A) Full network of sequences obtained via a BLAST search of the query sequence, Q0K1W7, after applying a minimum amino acid length of 250 and a maximum amino acid length of 800, resulting in 1,637 nodes, displayed using an alignment score of 60. Individual clusters are given a unique color. Our sequence of interest (Q0K1W7) is in cluster 2 (colored blue and light blue, where light blue nodes represent sequences predicted to function as 2,3-diketo-L-gulonate mutases). B) SSN of cluster 2 from panel A, displayed using an alignment score of 88. Coloring is identical to panel A.
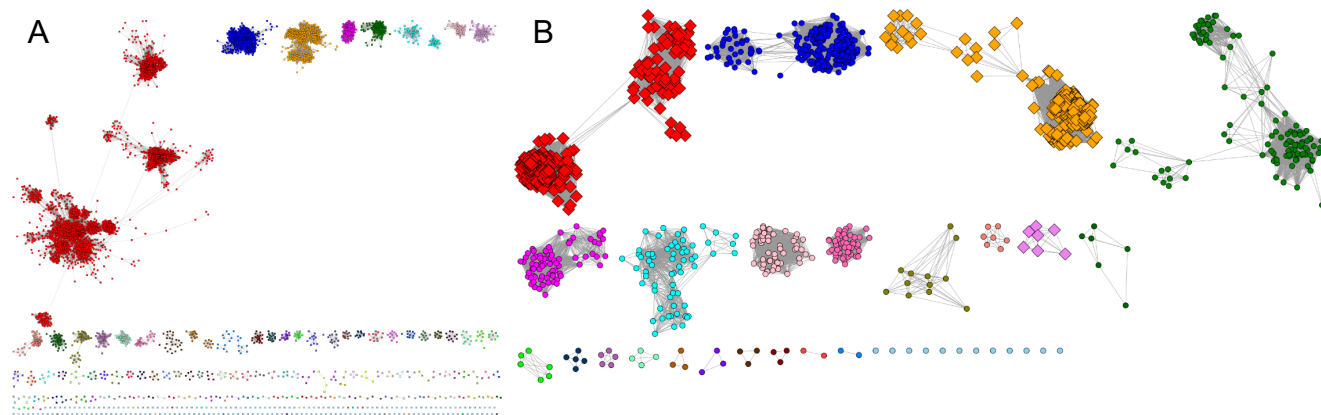
Figure S5. SSN analysis of PF04166 to find Q0K4Q7 (ClxD) homologues. A) UniRef90 network of PF04166, minimum length 275 amino acids, displayed using an alignment score of 85. Individual clusters are given a unique color. Our sequence of interest (Q0K4Q7) is in cluster 3 (colored orange). B) SSN of cluster 3 from panel A, displayed using an alignment score of 105. Individual clusters are given a unique color. Sequences that are predicted to function as 2-carboxy-L-lyxonate decarboxylases are shown as diamonds.

Figure S6. Genome neighborhood diagrams of *R. eutropha* and other organisms that share L-ascorbate catabolic genes.
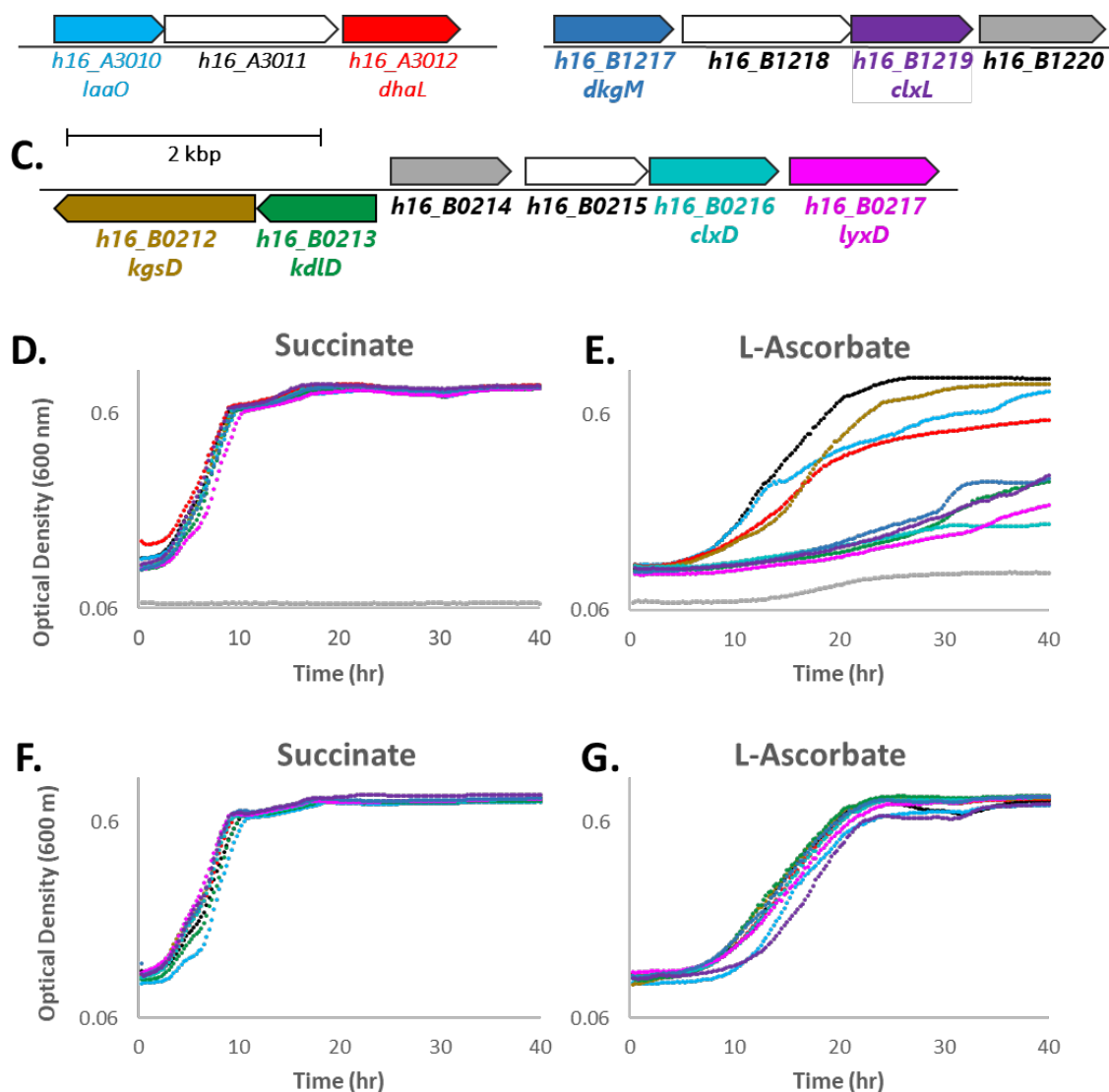
Figure S7. Growth of mutant and complemented mutant strains of *R. eutropha*. Genome neighborhoods from *R. eutropha* that encode module 1 (A), module 2 (B), and module 3 (C) of the L-ascorbate metabolic pathway. D, E) Growth with 10 mM of succinate (D) or L-ascorbate (E) of wild type (black) and mutant strains (colored) that are each missing a gene that is correspondingly colored from Panels A – C. The gray line represents spontaneous absorbance change of L-ascorbate in uninoculated media. F, G) Growth with 10 mM succinate (F) or L-ascorbate (G) of wild type containing pBBR1MCS2 (black) and mutant strains (colored) containing corresponding complementation plasmids. Some data is overlapping. Plasmid identities are described in **Supplementary Table S5**. Growth trends were similarly observed for biological and technical replicates of each strain.
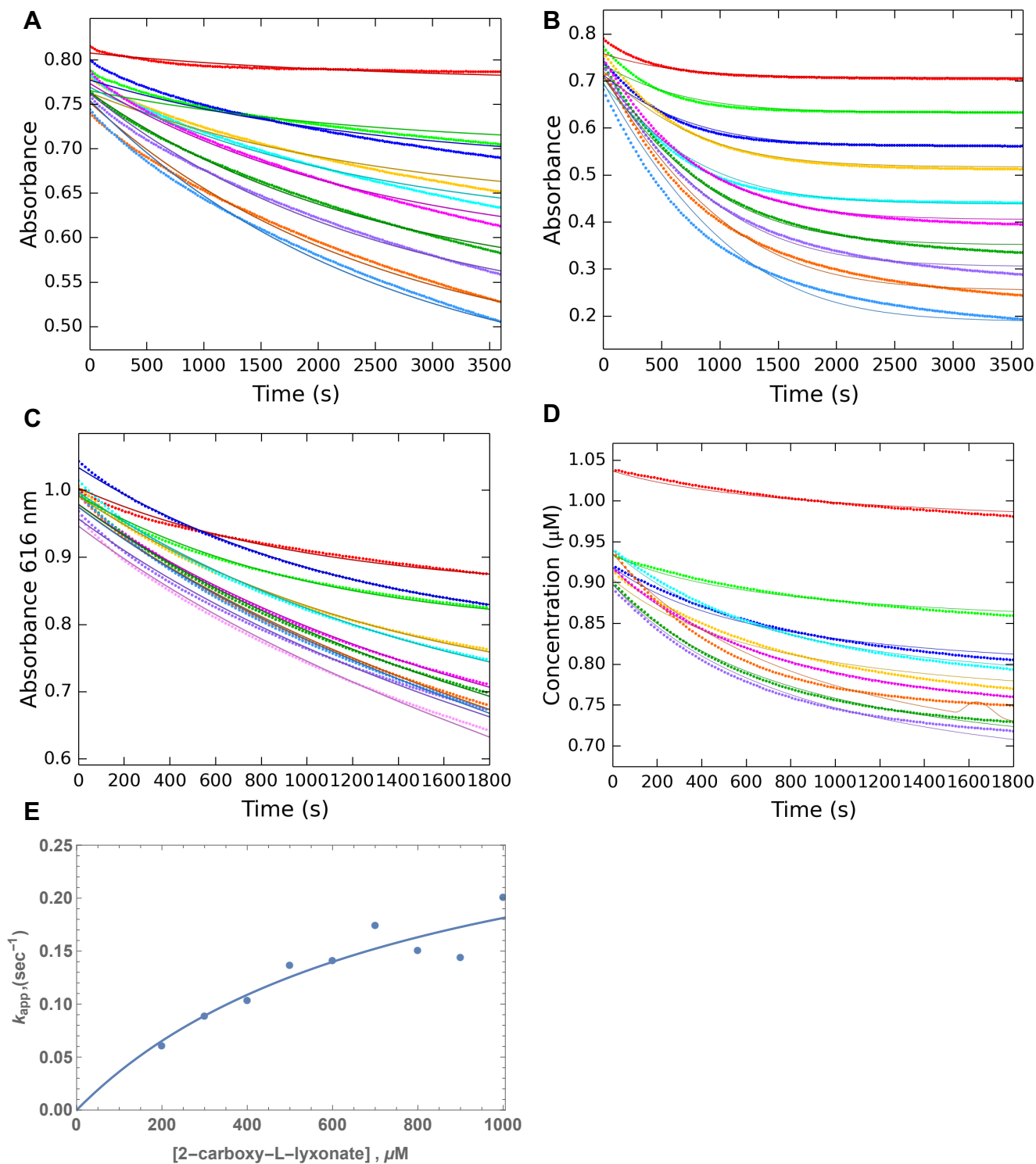
Figure S8. Raw kinetic data plots. A) Nonenzymatic L-dehydroascorbate (DHA) hydrolysis. DHA = 100, 200, 300, 400, 500, 600, 700, 800, 900, 1000 μM. B) DhaL data and fit. DhaL = 90 nM. DHA = 100, 200, 300, 400, 500, 600, 700, 800, 900, 1000 μM C) DkgM data and fit. DkgM = 0.1 μM, 2,3-diketo-L-gulonate = 0, 75, 150, 225, 300, 400, 500, 600, 700, 800, 1000 μM. D) ClxL data and fit. ClxL = 65 nM, 2-carboxy-L-lyxonolactone = 100, 200, 400, 500, 600, 700, 800, 900, 1000 μM. E) ClxD averaged triplicate data and fit. ClxD = 2 μM. 2-carboxy-L-lyxonate = 200, 300, 400, 500, 600, 700, 800, 900, 1000 μM.

S19
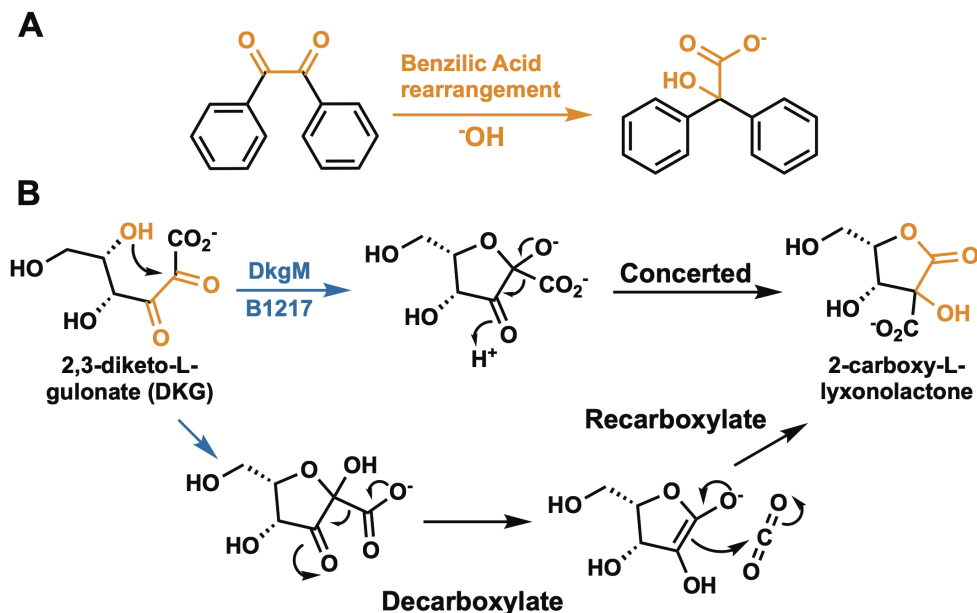
Figure S9. Benzilic acid rearrangement and potential mechanisms of DkgM. A) The base-catalyzed rearrangement of benzil leads to the conversion of a 1,2-diketone to the 2-hydroxy-carboxylate, benzilic acid. B) DkgM catalyzes the intramolecular attack of the C5 hydroxyl group in place of an hydroxide ion to convert the diketone 2,3-diketo-L-gulonate into the 2-hydroxy-lactone 2-carboxy-L-lyxonolactone. This may occur in a concerted migration of the carboxylate, or through a formal stepwise reaction involving decarboxylation and subsequent recarboxylation to the neighboring carbon atom.
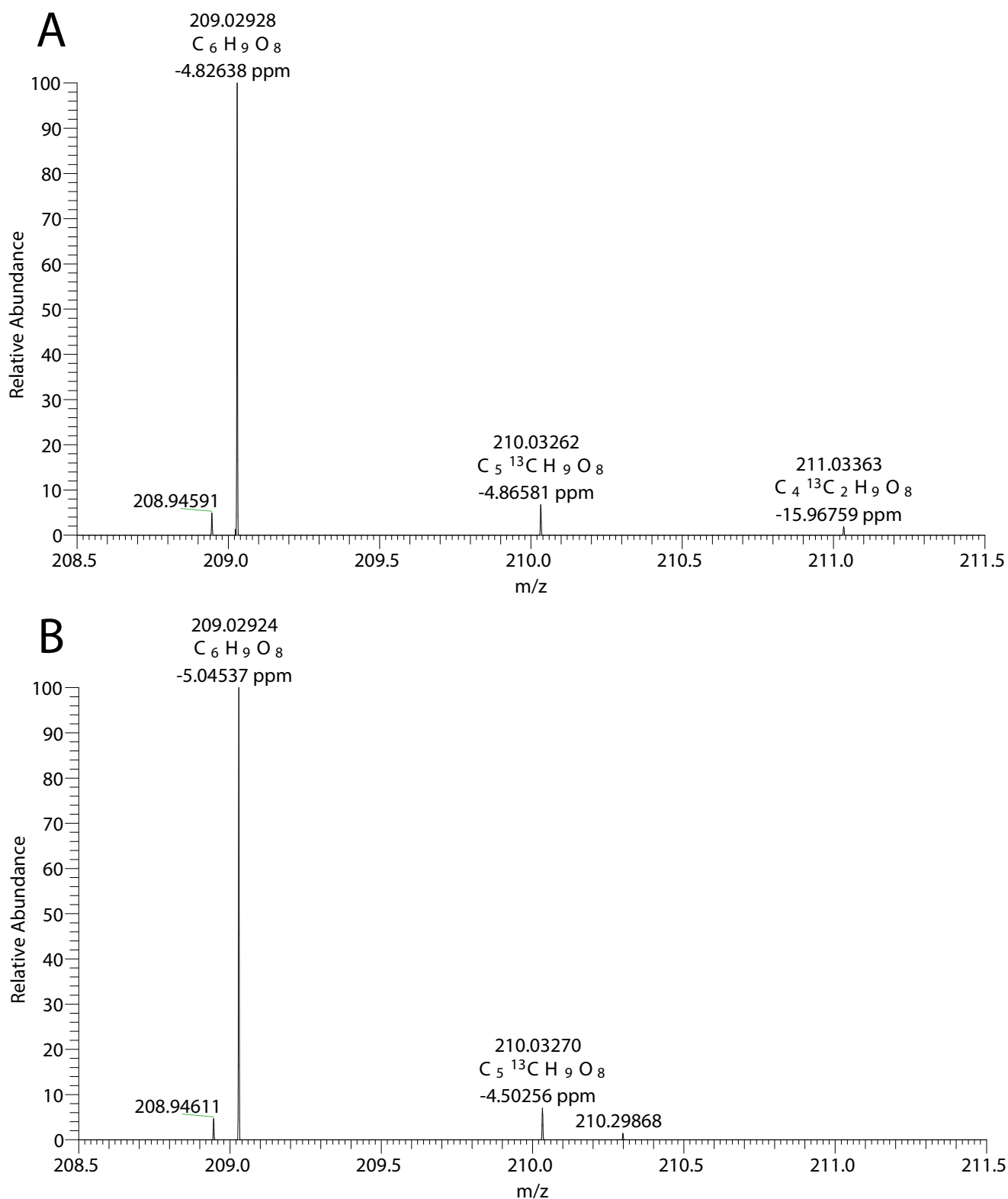
Figure S10. Example mass spectra of nonenzymatic DKG conversion to Clx. The relative abundances of Clx ($C_6H_9O_8^-$) and ^{13}C-labeled Clx ($C_5^{13}CH_9O_8^-$) are shown in the A) reaction incubated with sodium bicarbonate and B) reaction incubated with sodium [^{13}C]-bicarbonate.
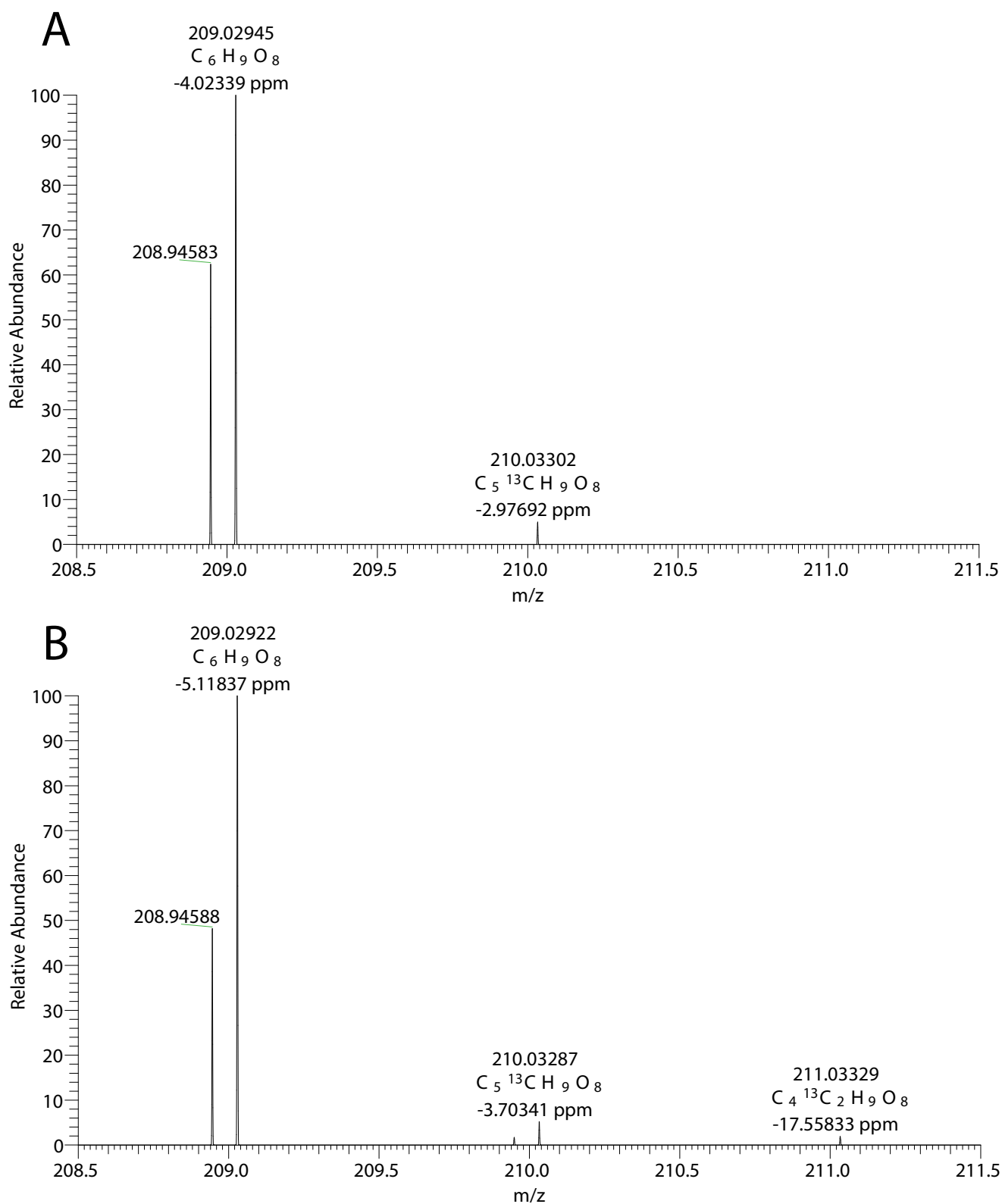
Figure S11. Example mass spectra of DkgM-catalyzed DKG conversion to Clx. The relative abundances of Clx ($C_6H_9O_8^-$) and ^{13}C-labeled Clx ($C_5^{13}CH_9O_8^-$) are shown in the A) reaction incubated with sodium bicarbonate and B) reaction incubated with sodium [^{13}C]-bicarbonate.
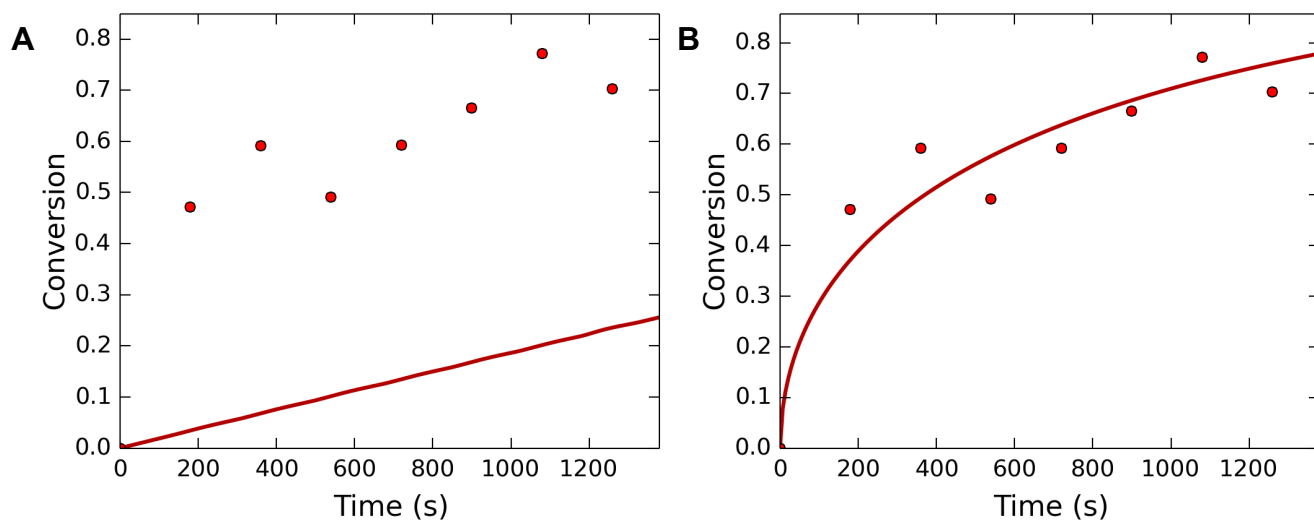
Figure S12. Plots of conversion of 2-carboxy-L-lyxonate to L-lyxonate by ClxD.
Experimental details described under "^{1}H NMR Full Kinetic Time Course of ClxD Reaction." A) Fit to the experimental data using the kinetics constants (k_{cat} = 0.33 ± 0.08 s^{-1}, K_m = 800 ± 400 µM, k_{cat}/K_m = 4.0 ± 2.0 × 10^2 M^{-1}s^{-1}) as determined by the coupled assay. B) Best fit to the experimental data by changing the k_{cat} value (k_{cat} = 180 s^{-1}, K_m = 800 µM, k_{cat}/K_m = 2.2 × 10^5 M^{-1}s^{-1}) of the coupled assay.
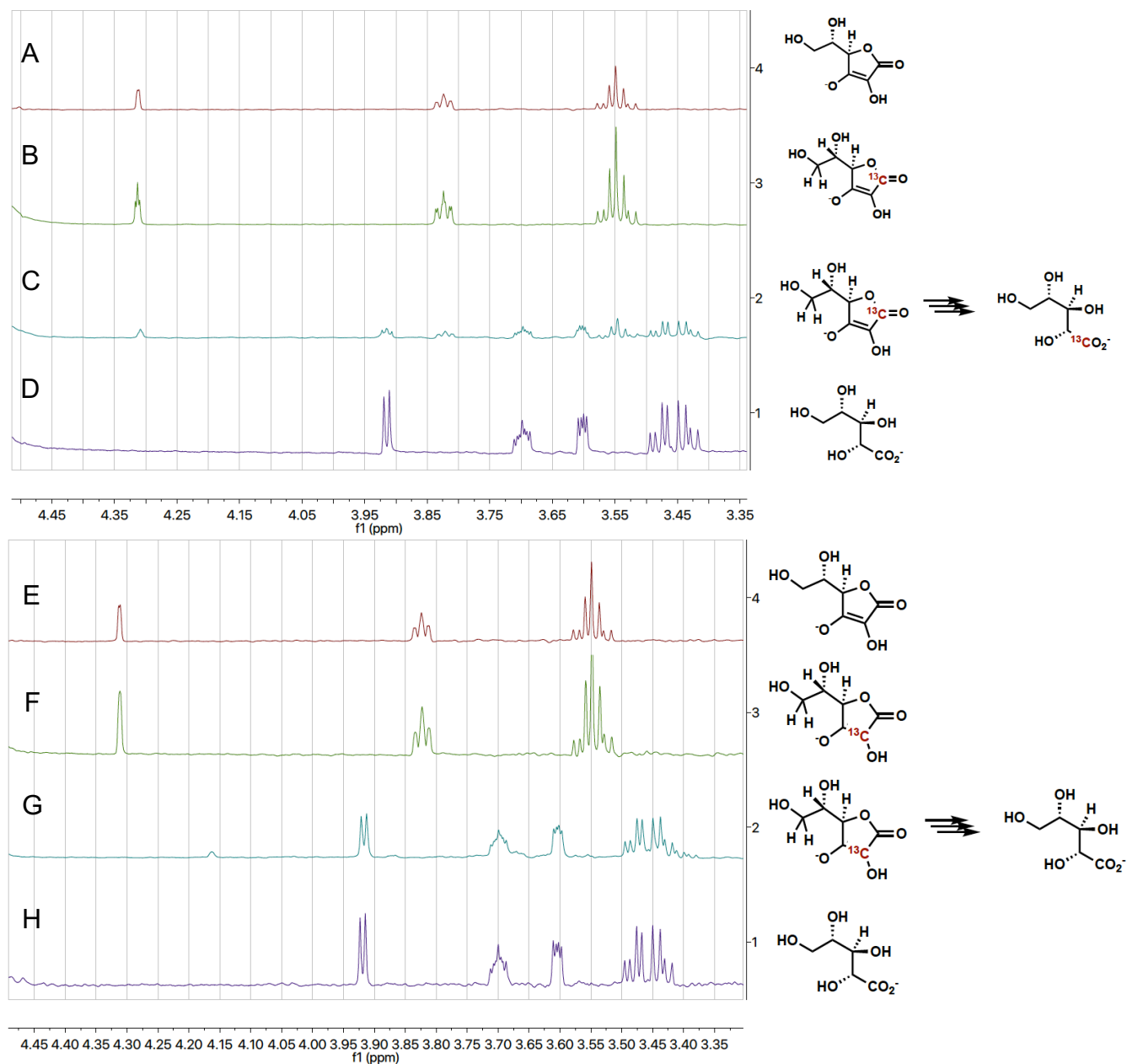
Figure S13. Aligned ^{1}H NMR spectra of coupled assays with [^{13}C]-labeled-L-ascorbate. ^{1}H NMR spectra of A) L-ascorbate, B) 1-[^{13}C]-L-ascorbate, C) the reaction after incubation of 1-[^{13}C]-L-ascorbate with DkgM, ClxL, and ClxD, D) L-lyxonate, E) L-ascorbate, F) 2-[^{13}C]-L-ascorbate, G) the reaction after incubation of 2-[^{13}C]-L-ascorbate with DkgM, ClxL, and ClxD, and H) L-lyxonate.
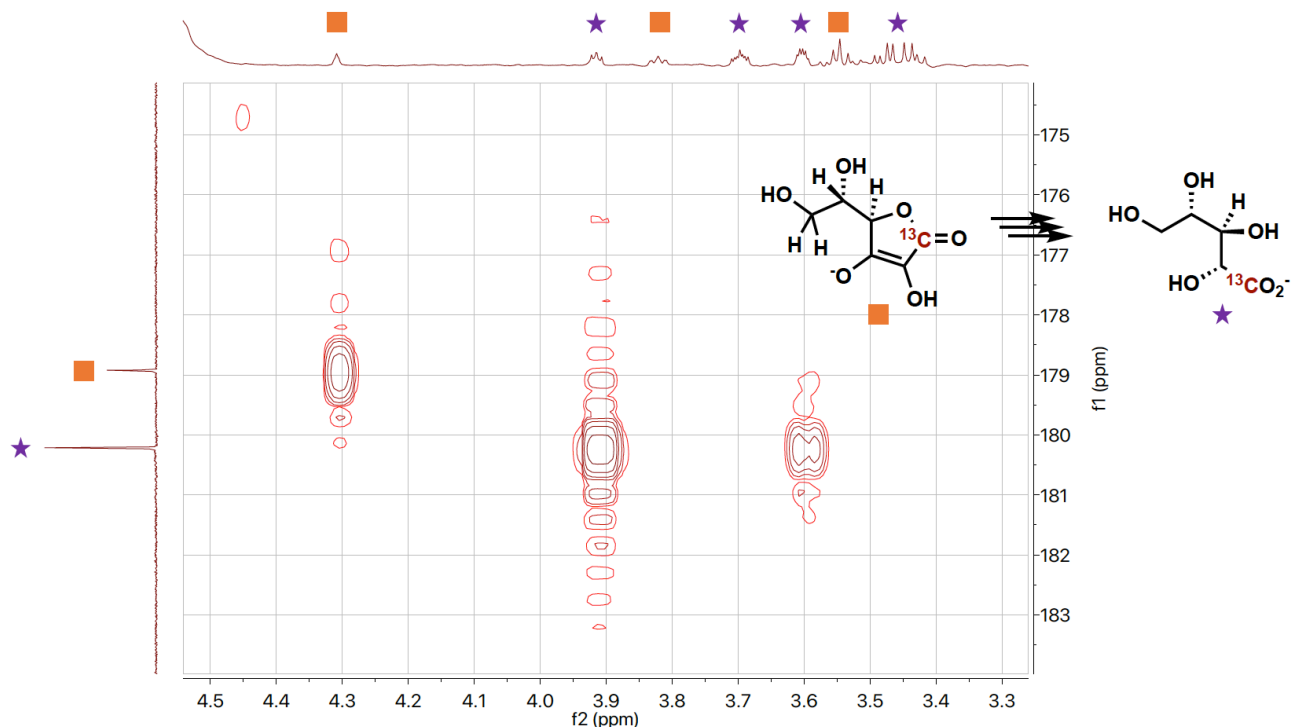
Figure S14. ^{1}H-^{13}C HMBC NMR of the reaction after incubation of 1-[^{13}C]-L-ascorbate with DkgM, ClxL, and ClxD.
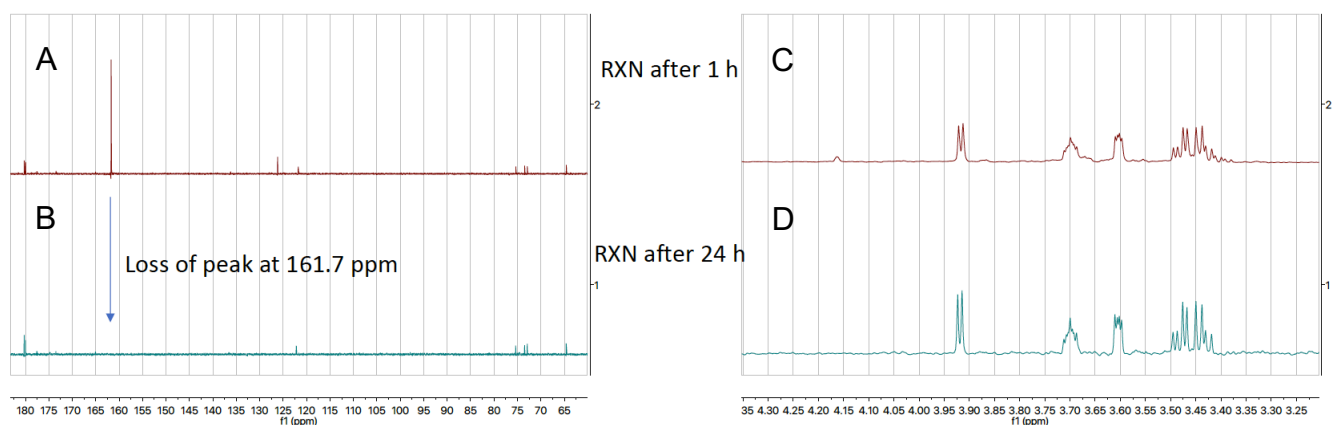
Figure S15. Aligned NMR spectra of 2-[^{13}C]-L-ascorbate reactions. Shown are the aligned ^{13}C NMR of A) the reaction after incubation of 2-[^{13}C]-L-ascorbate with ascorbate oxidase, DkgM, ClxL, and ClxD, after 1 h, and B) the same reaction after 24 h. Aligned ^{1}H NMR of C) the reaction after incubation of 2-[^{13}C]-L-ascorbate with ascorbate oxidase, DkgM, ClxL, and ClxD, after 1 h, and D) the same reaction after 24 h.
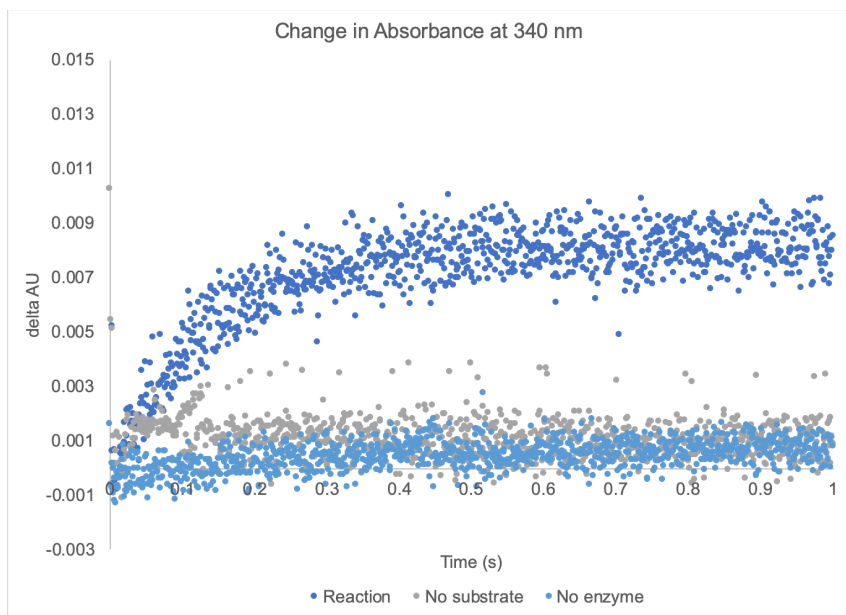
Figure S16. Stopped-flow absorbance measurement at 340 nm during the incubation of ClxD with Clx, compared to no substrate and no enzyme controls.
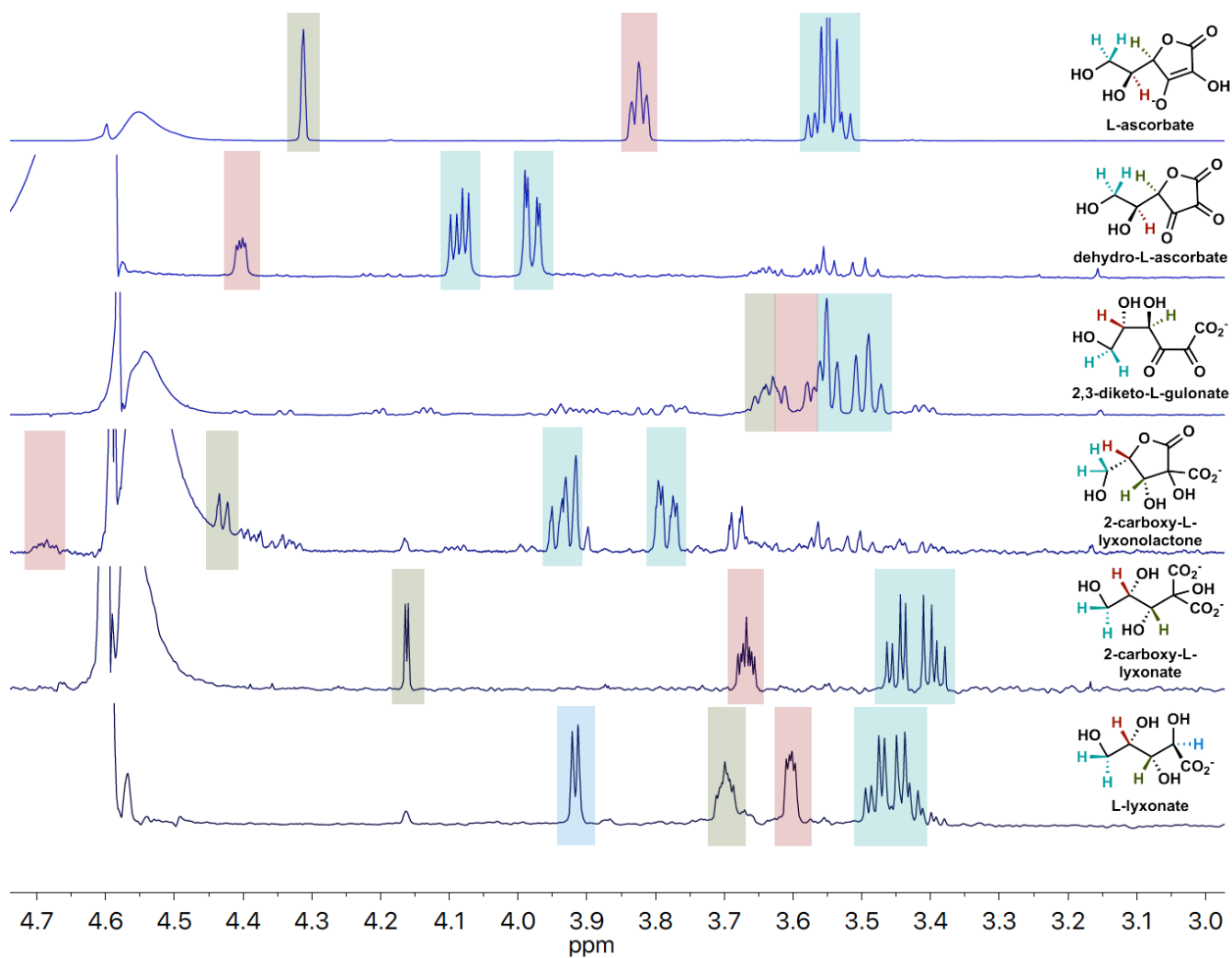
Figure S17. Aligned ^{1}H NMR spectra of pathway intermediates from L-ascorbate to L-lyxonate.

Supplementary References

(1)   Yew, W. S.; Fedorov, A. A.; Fedorov, E. V.; Rakus, J. F.; Pierce, R. W.; Almo, S. C.; Gerlt, J. A. Evolution of Enzymatic Activities in the Enolase Superfamily: L-Fuconate Dehydratase from Xanthomonas Campestris,. *Biochemistry* **2006**, *45* (49), 14582–14597. https://doi.org/10.1021/bi061687o.

(2)   Schäfer, A.; Tauch, A.; Jäger, W.; Kalinowski, J.; Thierbach, G.; Pühler, A. Small Mobilizable Multi-Purpose Cloning Vectors Derived from the Escherichia Coli Plasmids PK18 and PK19: Selection of Defined Deletions in the Chromosome of Corynebacterium Glutamicum. *Gene* **1994**, *145* (1), 69–73. https://doi.org/10.1016/0378-1119(94)90324-7.

(3)   Kovach, M. E.; Elzer, P. H.; Steven Hill, D.; Robertson, G. T.; Farris, M. A.; Roop, R. M.; Peterson, K. M. Four New Derivatives of the Broad-Host-Range Cloning Vector PBBR1MCS, Carrying Different Antibiotic-Resistance Cassettes. *Gene* **1995**, *166* (1), 175–176. https://doi.org/10.1016/0378-1119(95)00584-1.

(4)   Studier, F. W. Protein Production by Auto-Induction in High-Density Shaking Cultures. *Protein Expression and Purification* **2005**, *41* (1), 207–234. https://doi.org/10.1016/j.pep.2005.01.016.

(5)   Hobbs, M. E.; Vetting, M.; Williams, H. J.; Narindoshvili, T.; Kebodeaux, D. M.; Hillerich, B.; Seidel, R. D.; Almo, S. C.; Raushel, F. M. Discovery of an L-Fucono-1,5-Lactonase from Cog3618 of the Amidohydrolase Superfamily. *Biochemistry* **2013**, *52* (1), 239–253. https://doi.org/10.1021/bi3015554.

(6)   Johnson, K. A. Chapter 23 Fitting Enzyme Kinetic Data with KinTek Global Kinetic Explorer. In *Methods in Enzymology*; Johnson, M. L., Brand, L., Eds.; Computer Methods Part B; Academic Press, 2009; Vol. 467, pp 601–626. https://doi.org/10.1016/S0076-6879(09)67023-3.

(7)   Zhang, X.; Carter, M. S.; Vetting, M. W.; San Francisco, B.; Zhao, S.; Al-Obaidi, N. F.; Solbiati, J. O.; Thiaville, J. J.; de Crécy-Lagard, V.; Jacobson, M. P.; et al. Assignment of Function to a Domain of Unknown Function: DUF1537 Is a New Kinase Family in Catabolic Pathways for Acid Sugars. *Proc. Natl. Acad. Sci. U.S.A.* **2016**, *113* (29), E4161-4169. https://doi.org/10.1073/pnas.1605546113.
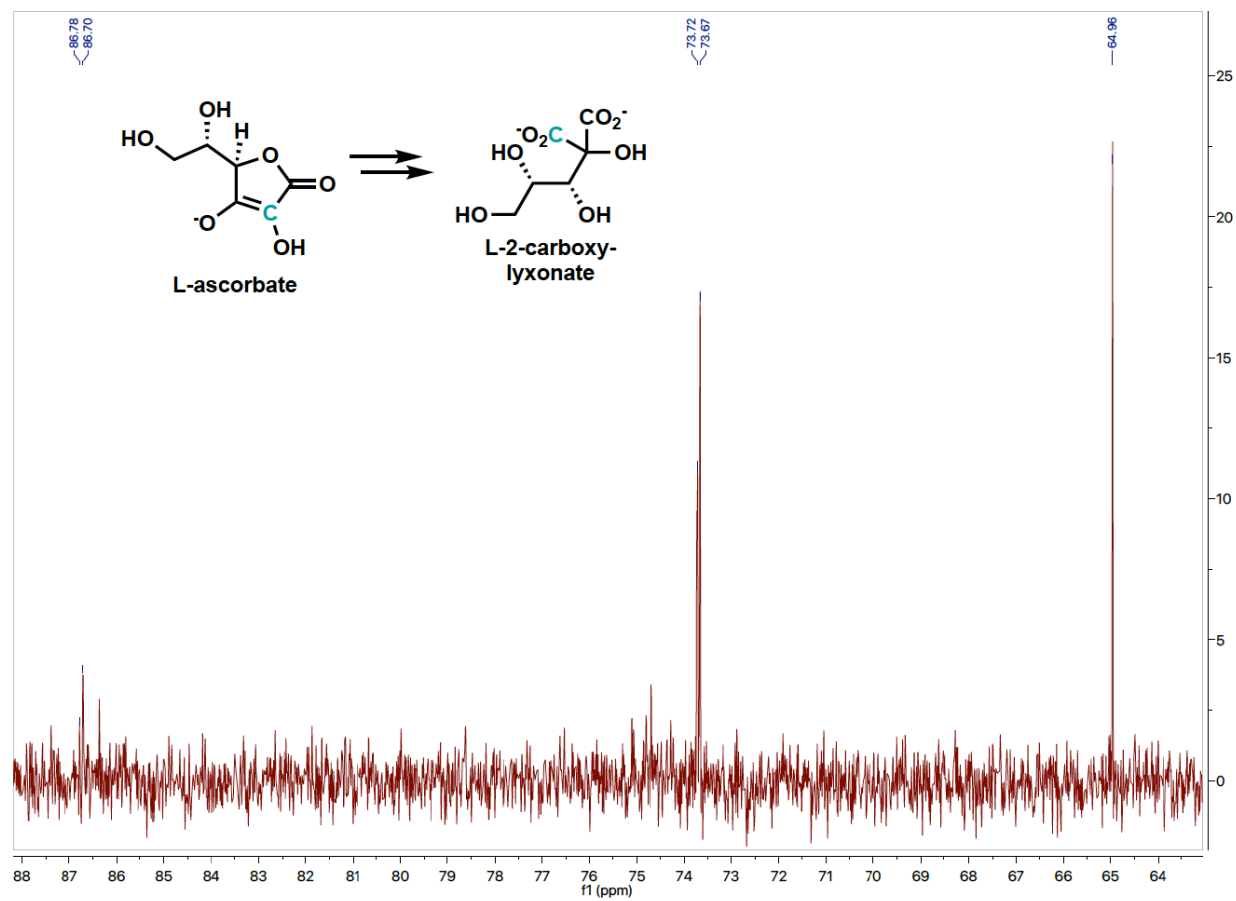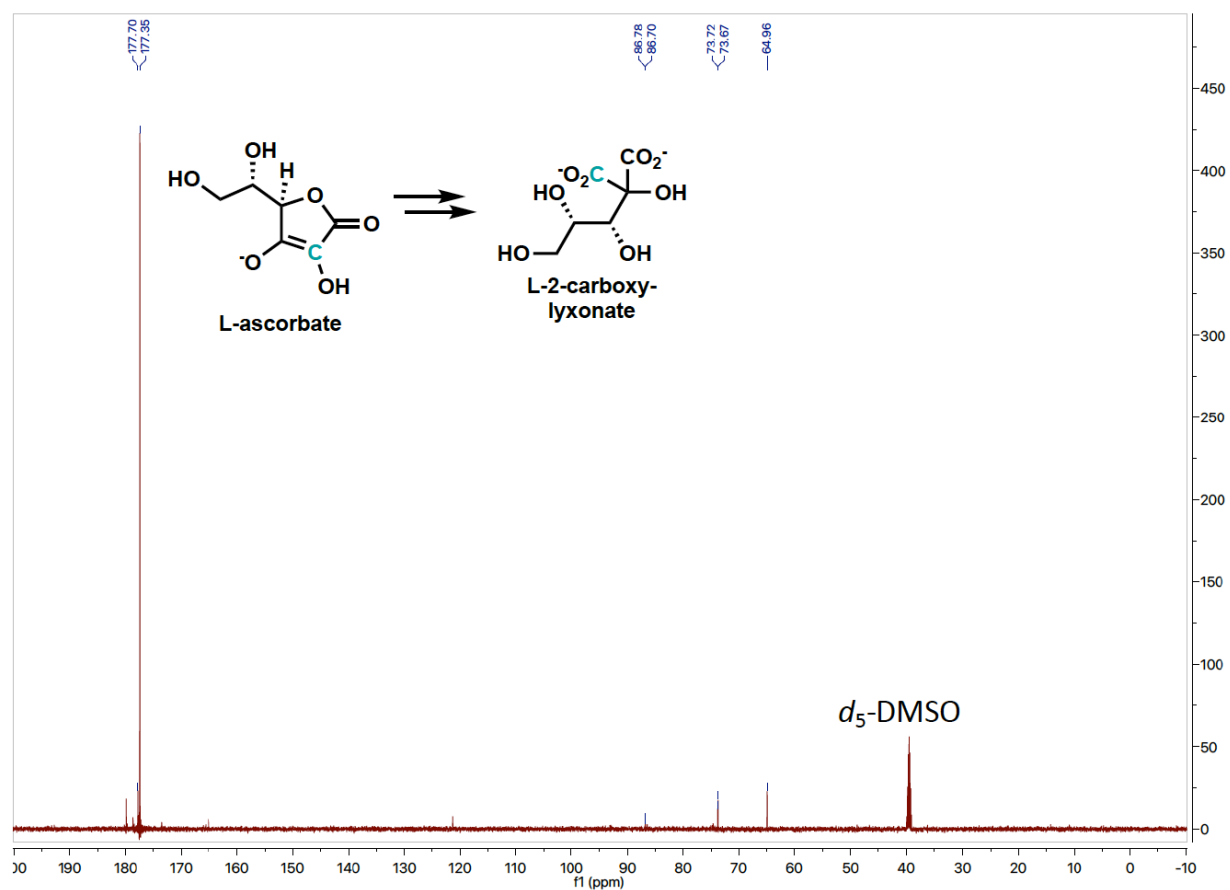
Full and Expanded NMR Spectra
2-carboxy-L-lyxonolactone, ^{1}H NMR (600 MHz, 50% D_2O pH 7.2)
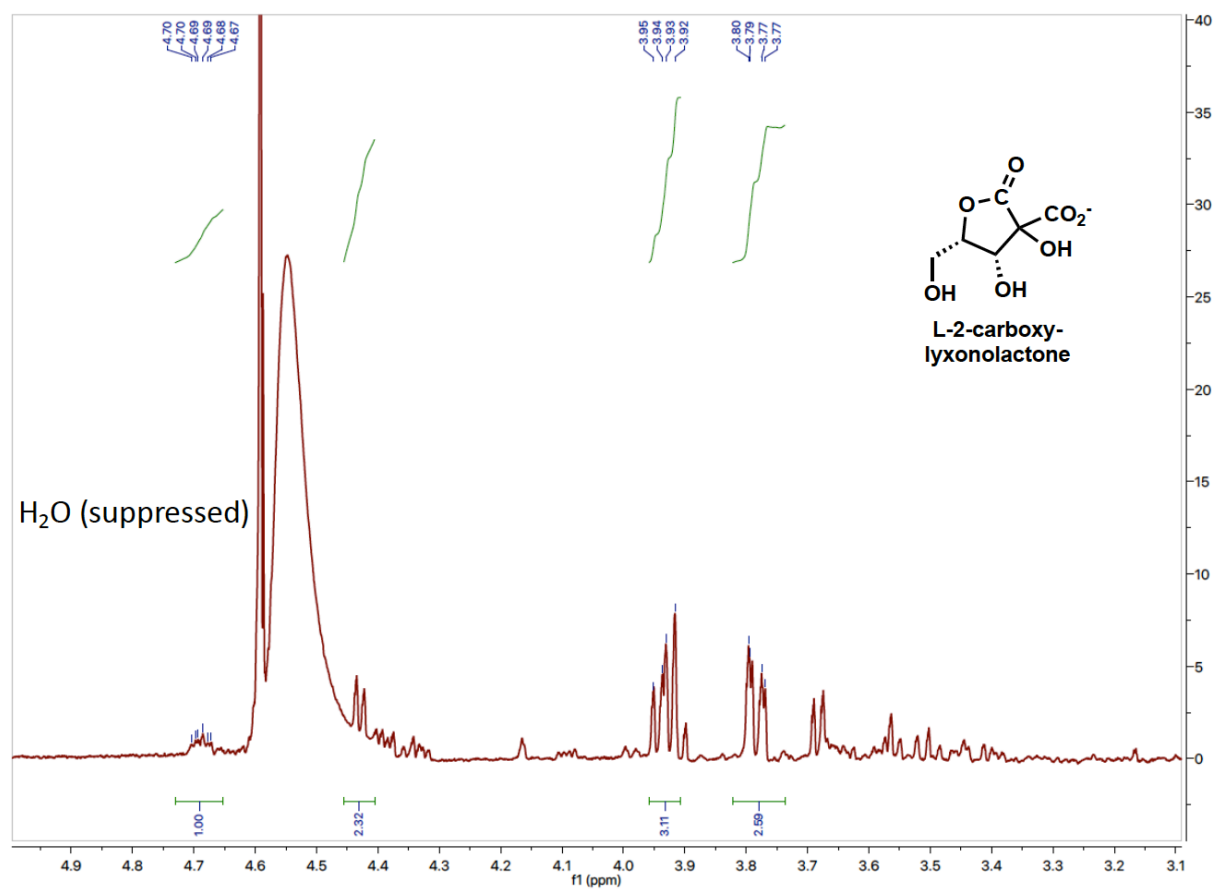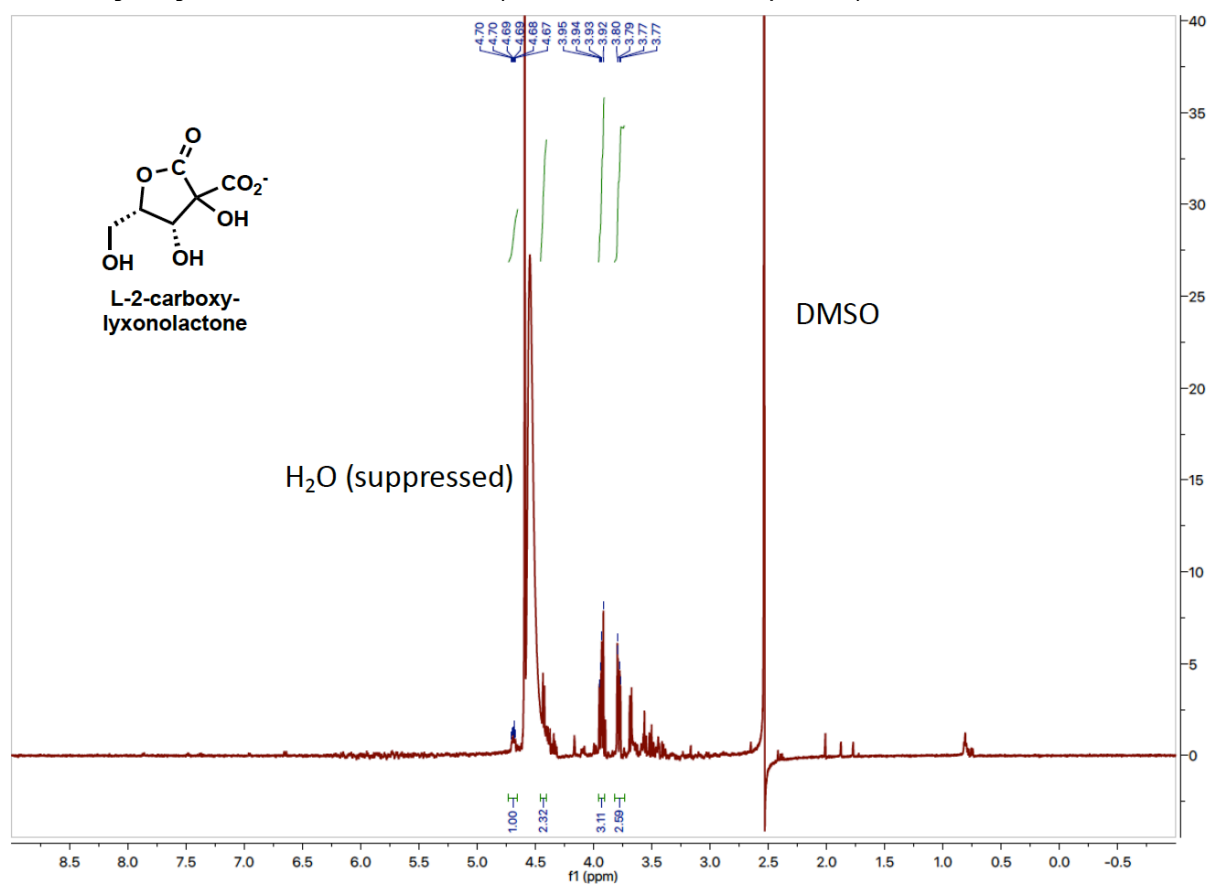
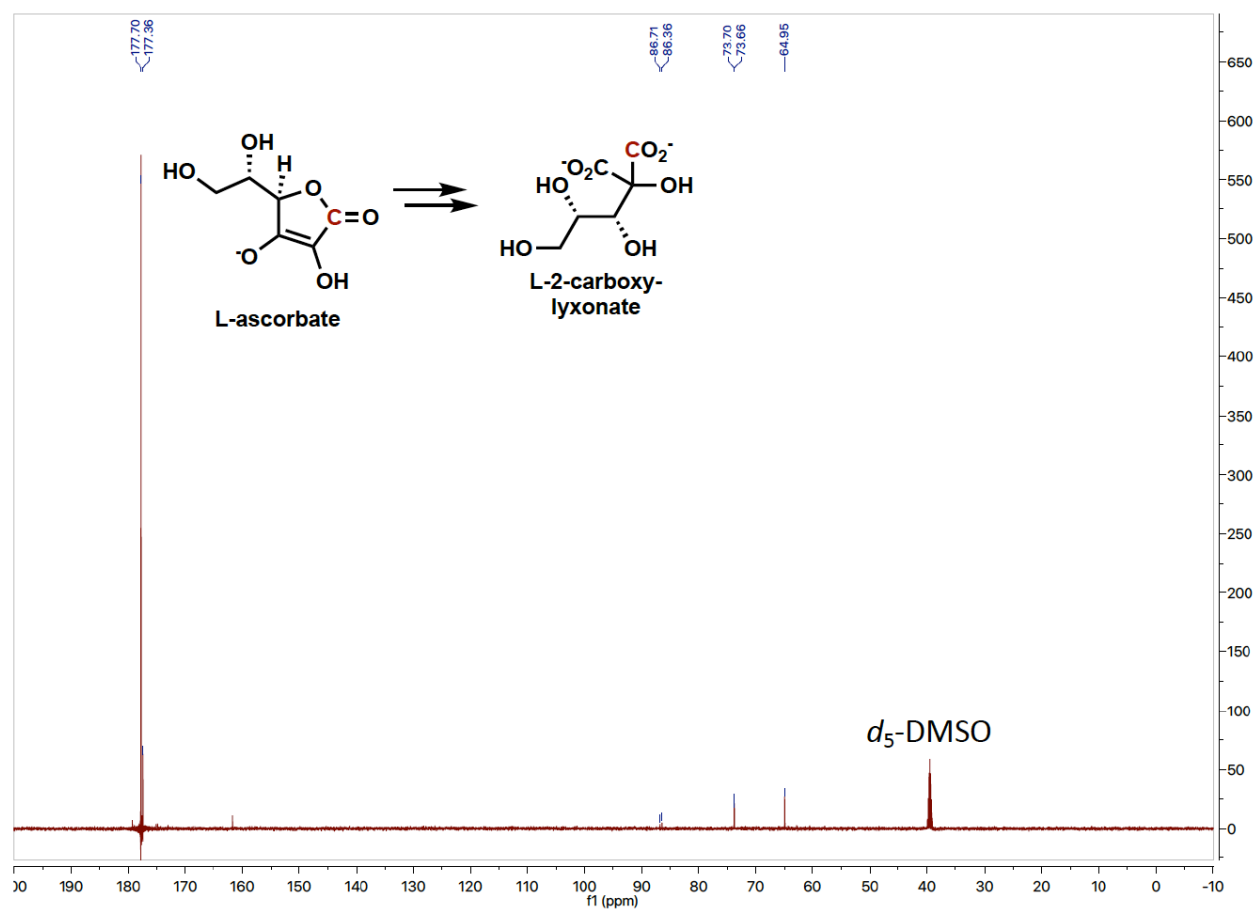**2-carboxy-L-lyxonate, ^{1}H NMR** (600 MHz, H_2O pH 7.2 5% DMSO-d_6)
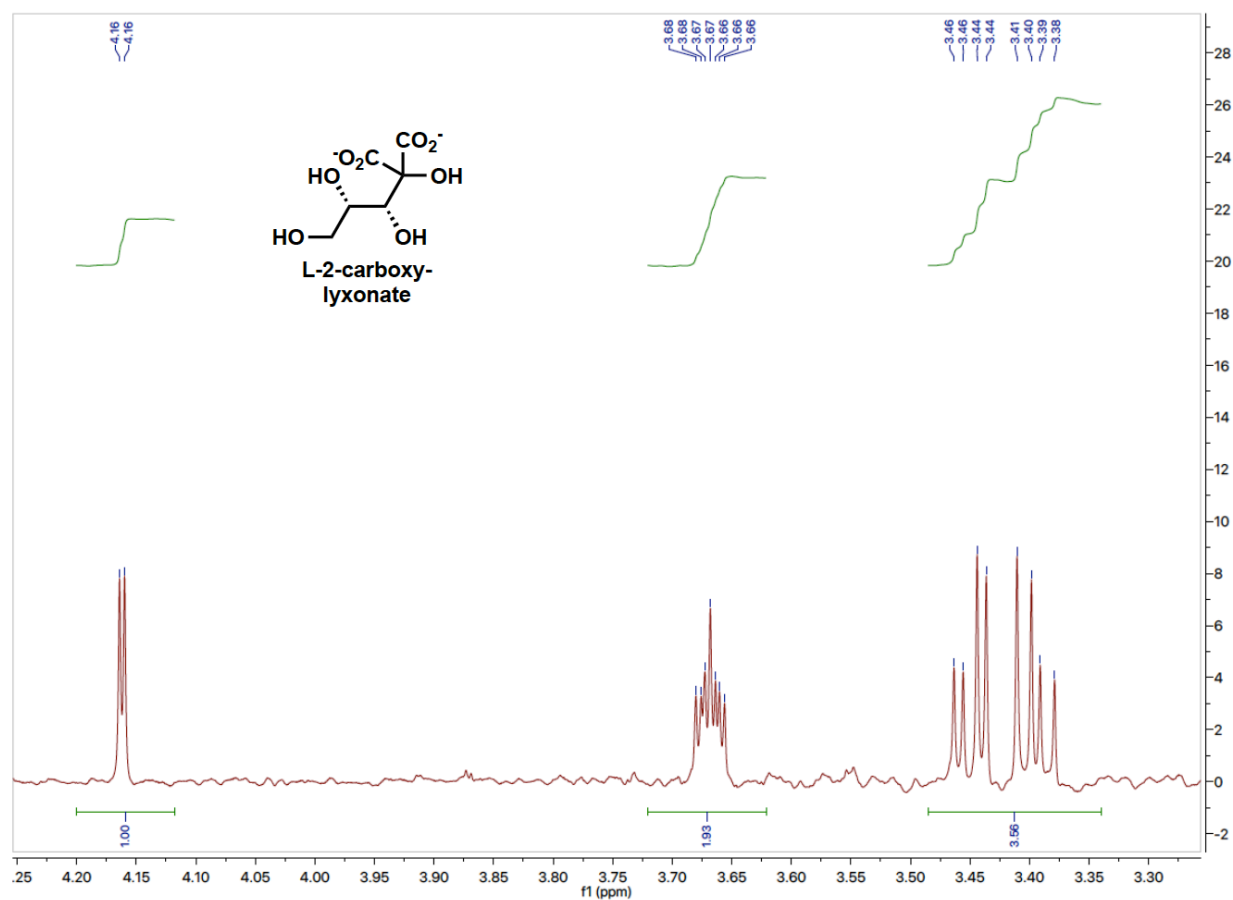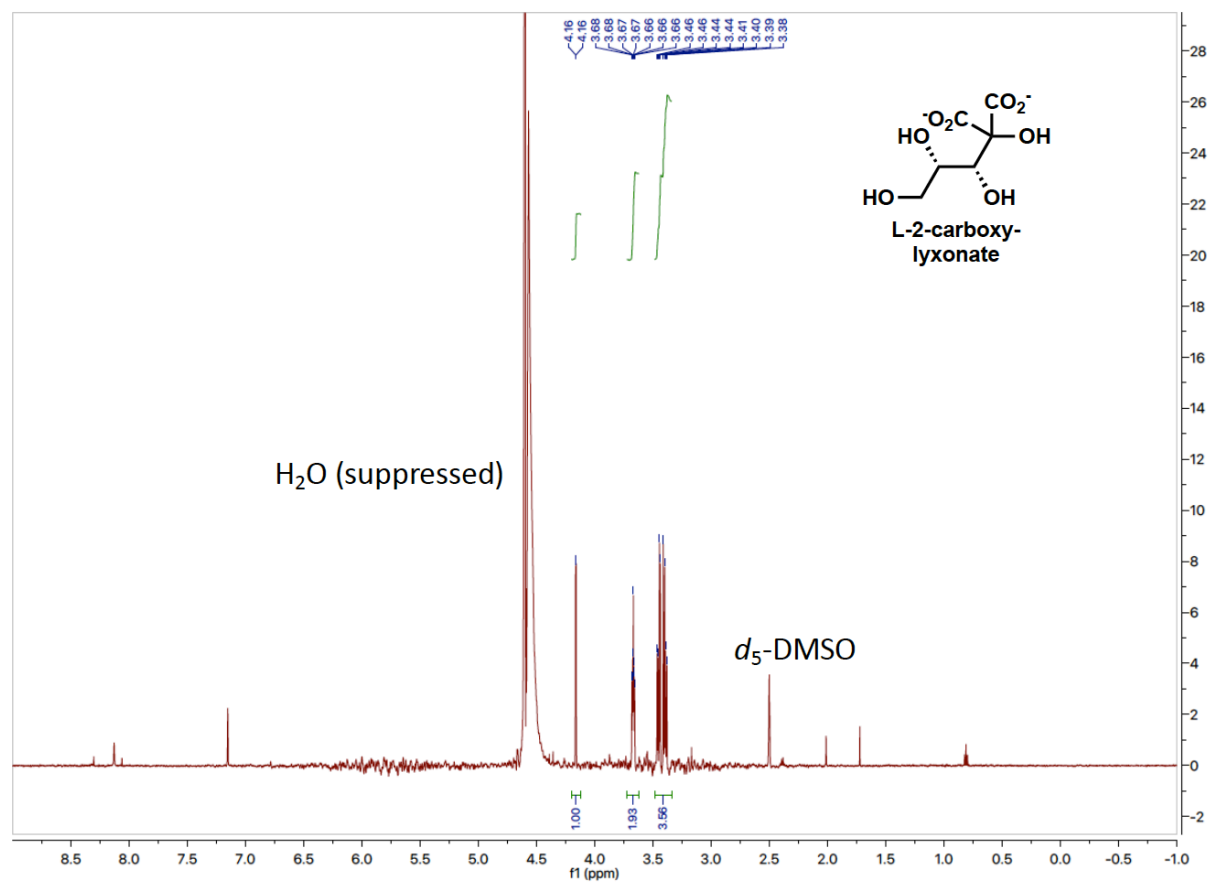
2-[^{13}C]-2-carboxy-L-lyxonolactone, ^{13}C NMR (150 MHz, H$_2$O pH 7.2 5% DMSO-d_6)

1-[^{13}C]-2-carboxy-L-lyxonolactone, ^{13}C NMR (150 MHz, H$_2$O pH 7.2 5% DMSO-d_6)

2-carboxy-L-lyxonolactone, ^{13}C NMR (150 MHz, H_2O pH 7.2 5% DMSO-d_6)

L-2-carboxy-lyxonate

imidazole

d_5-DMSO